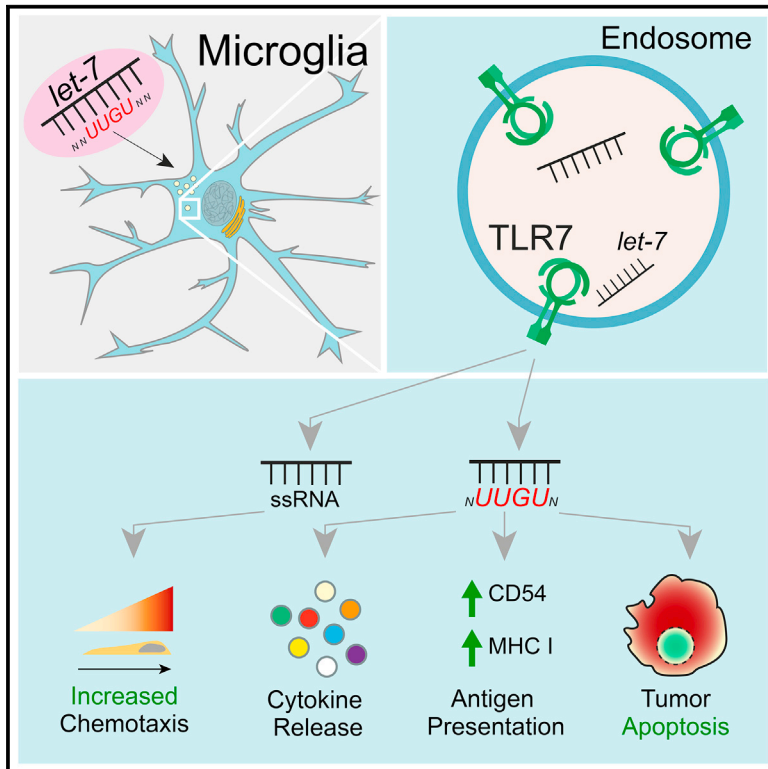# *let-7* MicroRNAs Regulate Microglial Function and Suppress Glioma Growth through Toll-Like Receptor 7

Graphical Abstract

Authors

Alice Buonfiglioli, Ibrahim E. Efe, Dilansu Guneykaya, ..., Marcus Semtner, Helmut Kettenmann, Seija Lehnardt

Correspondence

kettenmann@mdc-berlin.de (H.K.), seija.lehnardt@charite.de (S.L.)

In Brief

Buonfiglioli et al. elucidate the role of *let-7* miRNAs acting as Toll-like receptor (TLR) ligands in the brain. Select *let-7* miRNAs function as signaling molecules to modulate diverse microglial functions and glioma growth through TLR7. These data establish *let-7* miRNAs as TLR7 signaling activators of microglia in health and glioma.

Highlights

- *let-7* miRNAs act as Toll-like receptor (TLR) 7 signaling molecules in glioma

- Extracellular *let-7* miRNAs differentially modulate microglial biology

- The sequence motif UUGU is responsible for *let-7*-induced microglial activation

- Select *let-7* miRNAs attenuate glioma growth by directly activating microglial TLR7

let-7 MicroRNAs Regulate Microglial Function and Suppress Glioma Growth through Toll-Like Receptor 7

Alice Buonfiglioli,[1,2] Ibrahim E. Efe,[2,3] Dilansu Guneykaya,[2] Andranik Ivanov,[4] Yimin Huang,[2] Elisabeth Orlowski,[2] Christina Krüger,[1] Rudolf A. Deisz,[1] Darko Markovic,[5] Charlotte Flüh,[6] Andrew G. Newman,[1] Ulf C. Schneider,[7] Dieter Beule,[4,8] Susanne A. Wolf,[9] Omar Dzaye,[3,10] David H. Gutmann,[11] Marcus Semtner,[2] Helmut Kettenmann,[2,13,*] and Seija Lehnardt[1,12,13,14,*]

[1]Institute of Cell Biology and Neurobiology, Charité – Universitätsmedizin Berlin, corporate member of Freie Universität Berlin, Humboldt-Universität zu Berlin, and Berlin Institute of Health, 10117 Berlin, Germany
[2]Department of Cellular Neurosciences, Max-Delbrueck-Center for Molecular Medicine in the Helmholtz Association, 13125 Berlin, Germany
[3]Department of Radiology, Charité – Universitätsmedizin Berlin, corporate member of Freie Universität Berlin, Humboldt-Universität zu Berlin, and Berlin Institute of Health, 10117 Berlin, Germany
[4]Core Unit Bioinformatics, Berlin Institute of Health, Charité – Universitätsmedizin Berlin, corporate member of Freie Universität Berlin, Humboldt-Universität zu Berlin, and Berlin Institute of Health, 10117 Berlin, Germany
[5]Department of Neurosurgery, Helios Clinics, 13125 Berlin, Germany
[6]Department of Neurosurgery, University Medical Center Schleswig-Holstein (UKSH), 24105 Kiel, Germany
[7]Department of Neurosurgery, Charité – Universitätsmedizin Berlin, corporate member of Freie Universität Berlin, Humboldt-Universität zu Berlin, and Berlin Institute of Health, 10117 Berlin, Germany
[8]Max-Delbrueck-Center for Molecular Medicine in the Helmholtz Association, Berlin, Germany
[9]Department of Ophthalmology, Charité – Universitätsmedizin Berlin, corporate member of Freie Universität Berlin, Humboldt-Universität zu Berlin, and Berlin Institute of Health, 10117 Berlin, Germany
[10]Russell H. Morgan Department of Radiology and Radiological Science, Johns Hopkins University School of Medicine, Baltimore, MD, USA
[11]Department of Neurology, Washington University School of Medicine, St. Louis, MO 63110, USA
[12]Department of Neurology, Charité – Universitätsmedizin Berlin, corporate member of Freie Universität Berlin, Humboldt-Universität zu Berlin, and Berlin Institute of Health, 10117 Berlin, Germany
[13]These authors contributed equally
[14]Lead Contact
*Correspondence: kettenmann@mdc-berlin.de (H.K.), seija.lehnardt@charite.de (S.L.)
https://doi.org/10.1016/j.celrep.2019.11.029

SUMMARY

Microglia express Toll-like receptors (TLRs) that sense pathogen- and host-derived factors, including single-stranded RNA. In the brain, *let-7* microRNA (miRNA) family members are abundantly expressed, and some have recently been shown to serve as TLR7 ligands. We investigated whether *let-7* miRNA family members differentially control microglia biology in health and disease. We found that a subset of *let-7* miRNA family members function as signaling molecules to induce microglial release of inflammatory cytokines, modulate antigen presentation, and attenuate cell migration in a TLR7-dependent manner. The capability of the *let-7* miRNAs to control microglial function is sequence specific, mapping to a *let-7* UUGU motif. In human and murine glioblastoma/glioma, *let-7* miRNAs are differentially expressed and reduce murine GL261 glioma growth in the same sequence-specific fashion through microglial TLR7. Taken together, these data establish *let-7* miRNAs as key TLR7 signaling activators that serve to regulate the diverse functions of microglia in health and glioma.

INTRODUCTION

MicroRNAs (miRNAs) are short, non-coding single-stranded RNA (ssRNA) molecules, shown to posttranscriptionally regulate gene expression (Bartel, 2004). The lethal-7 (*let-7*) miRNA family, the first miRNA family identified in humans (Pasquinelli et al., 2000), includes nine mature members (*let-7a–let-7i* and *miR-98*). *let-7* miRNAs, which are abundantly expressed in the brain and exhibit high cross-species sequence conservation (Pena et al., 2009; Reinhart et al., 2000), have been shown to regulate cell differentiation and brain tumor growth (Gilles and Slack, 2018; Lee et al., 2016). miRNAs are also present in the extracellular space, derived either from dying cells or actively released within vesicles (e.g., exosomes), where they function as signaling molecules (Feng et al., 2017; Lehmann et al., 2012a). Some miRNAs can serve as ligands for Toll-like receptors (TLRs) (Fabbri et al., 2012; Feng et al., 2017; Lehmann et al., 2012a). TLRs belong to a family of pattern recognition receptors, which recognize pathogen-associated molecules, such as bacterial and viral components, and damage-associated molecules derived from necrotic cells and tumor tissue (Tang et al., 2012). Upon activation, TLRs signal through a complex array of effector proteins resulting in inflammation (Kawai and Akira, 2006). Importantly, there is sequence specificity to miRNA engagement of TLRs, in that the GUUGUGU motif, found in *let-7b*, is required for TLR7 recognition of ssRNA40, a nucleotide derived from HIV (Heil et al., 2004).

Microglia respond to brain pathological states by migrating toward the lesion site, releasing inflammatory molecules, engulfing cell debris (Napoli and Neumann, 2009), and presenting disease-associated antigen, thereby contributing to CNS disease pathobiology (Wlodarczyk et al., 2014). Some of these responses are mediated by TLRs, such as TLR7, which detects ssRNA (Diebold et al., 2004; Heil et al., 2004) and controls microglial chemotaxis (Ifuku et al., 2016). Additional TLRs regulate microglial motility (TLR2; Ifuku et al., 2016) and phagocytosis of Aβ amyloid in Alzheimer's disease (TLR4; Rajbhandari et al., 2014). In the setting of glioblastoma (GBM), the most aggressive brain tumor in adults with survival of less than 15 months from diagnosis (Louis et al., 2016; Stupp et al., 2005), TLR2 and TLR4 control the interaction between glioma cells and microglia, thereby promoting tumor expansion (Dzaye et al., 2016; Hu et al., 2015; Vinnakota et al., 2013). Glioma-associated microglia and invading peripheral macrophages constitute up to 30% of the tumor tissue, adopting a tumor-supportive phenotype (Hambardzumyan et al., 2016).

Here, we systematically analyzed the different members of the *let-7* miRNA family to determine which of these molecules function as microglial TLR signaling molecules. We found that a defined subset of the *let-7* miRNA family, characterized by a specific nucleotide sequence, activates TLR7 and modulates microglial release of inflammatory cytokines, migration, and antigen presentation. This selectivity operates in the setting of GBM, in which select *let-7* miRNAs inhibit tumor growth via microglial TLR7 signaling. Our data establish that *let-7* miRNA dictates microglial function through TLR7 signaling, which is important for physiological and pathological processes in the CNS.

RESULTS AND DISCUSSION

Select Members of the *let-7* miRNA Family Activate Microglia via TLR7 Signaling

Microglia are the resident immune cells of the CNS, where they function as sensors of changes in their environment caused by invading pathogens and host-derived factors. Following activation, microglia migrate to the lesion site and secrete cytokines and chemokines (Kettenmann et al., 2011). These responses are regulated in part by TLRs. Consistent with a central role for TLRs in brain homeostasis, miRNAs serve as TLR signaling activators (Fabbri et al., 2012; Feng et al., 2017; He et al., 2013; Lehmann et al., 2012a). miRNA dysregulation is linked to inflammatory and immune responses, which modulate cancer initiation and progression (Gilles and Slack, 2018). On the basis of sequence similarity to known TLR7 ligands, such as the oligoribonucleotide ssRNA40 derived from HIV, their abundant expression in the CNS, and their key role in immune responses in pathology including cancer, we focused on the *let-7* miRNA family members as potential signaling activators of microglia in health and in the setting of GBM. To this end, first we sought to systematically investigate the potential of different *let-7* miRNA family members (Table S1) to activate TLR7 in microglia. Cultured microglia from neonatal wild-type (WT) mice were incubated for 9, 24, and 30 h with synthetic oligoribonucleotides derived from the *let-7* miRNA family at different concentrations (1, 5, and 10 μg/mL), and analyzed for TNF-α release using ELISA. Lipopolysaccharide (LPS) and loxoribine (LOX) served as positive controls for TLR4 and TLR7 activation, respectively. *let-7a*, *let-7b*, *let-7c*, *let-7e*, *let-7f*, and *let-7g* induced TNF-α release from microglia time- and dose-dependently (Figure 1A). There was increased TNF-α release after 24 h relative to 9 h, while after 30 h, at 5 μg/mL, there was no further increase. TNF-α release in response to 5 μg/mL *let-7* miRNA was higher compared with 1 μg/mL, but not much different at 10 μg/mL after 24 h. *let-7* miRNA-induced responses were sequence specific, as control oligoribonucleotides with a mutant sequence did not induce TNF-α release. In contrast to the responses triggered by the *let-7* miRNAs above, TNF-α induced by *let-7d*, *let-7i*, and *miR-98* was only slightly increased relative to control (Figure 1A). Using biotinylated *let-7b*, we confirmed that extracellularly delivered *let-7* miRNA enters microglia (Figure 1B). To determine whether TLR7 is required for microglial activation by *let-7* miRNAs, microglia from neonatal $Tlr7^{-/-}$ mice were investigated. In contrast to WT microglia, TLR7-deficient microglia failed to release amounts of TNF-α in response to stimulation with any of the members of the *let-7* miRNA family at 5 μg/mL within 24 h (Figure 1C). As expected, stimulation with LOX was abolished in $Tlr7^{-/-}$ mice, while LPS- and Pam2CSK4 (ligand for TLR2)-induced responses were unaffected. Stimulation of $Tlr7^{-/-}$ microglia with different doses (1, 5, or 10 μg/mL) of any of the *let-7* miRNAs within 24 h or with 5 μg/mL *let-7* miRNA over different time periods (9, 24, or 30 h) did not result in significant TNF-α production compared with control (Figure S1). To exclude the possibility that the effects were due to contamination with TLR4 and/or TLR2 ligands, such as LPS or lipoproteins, we tested microglia from $Tlr2^{-/-}$ and $Tlr4^{-/-}$ mice (Figure 1C). TLR2- and TLR4-deficient microglia released TNF-α in response to the same *let-7* family members that activated WT microglia. TNF-α release induced by LPS in TLR4-deficient microglia, and by the TLR2 agonist Pam2CSK4 in TLR2-deficient microglia, was abolished.

To test whether *let-7*-mediated activation of microglia depends on their developmental stage or the isolation procedure, we compared TNF-α release triggered by *let-7* family members in postnatal microglia cultures to microglia from adult tissue and freshly isolated adult microglia. Adult microglia were isolated from 8-week-old mice and were grown *in vitro* for 3 weeks. Freshly isolated microglia were obtained from 12-week-old mice via fluorescence-activated cell sorting (FACS) and were seeded overnight before stimulation. Cells were stimulated with the different *let-7* family members and analyzed using ELISA (Figure 2). Adult microglia and freshly isolated adult microglia released TNF-α in response to *let-7b*, *let-7c*, *let-7e*, *let-7f*, and *let-7g*. Compared with neonatal microglia, these responses were smaller in magnitude. As observed in neonatal microglia, adult microglia and freshly isolated adult microglia exhibited little TNF-α release in response to *let-7a*, *let-7d*, *let-7i*, or *miR-98* stimulation (Figure 2). These microglial responses were sequence specific, as control oligoribonucleotides with a mutant sequence did not induce TNF-α release. To confirm *let-7* miRNAs as signaling activators of immune cells, not only in the CNS but also in the periphery, we analyzed bone marrow-derived macrophages using the same experimental protocol. Monocytes were isolated from bone marrows of 8-week-old mice and differentiated into macrophages for 6 days. We observed a sequence-specific release of TNF-α
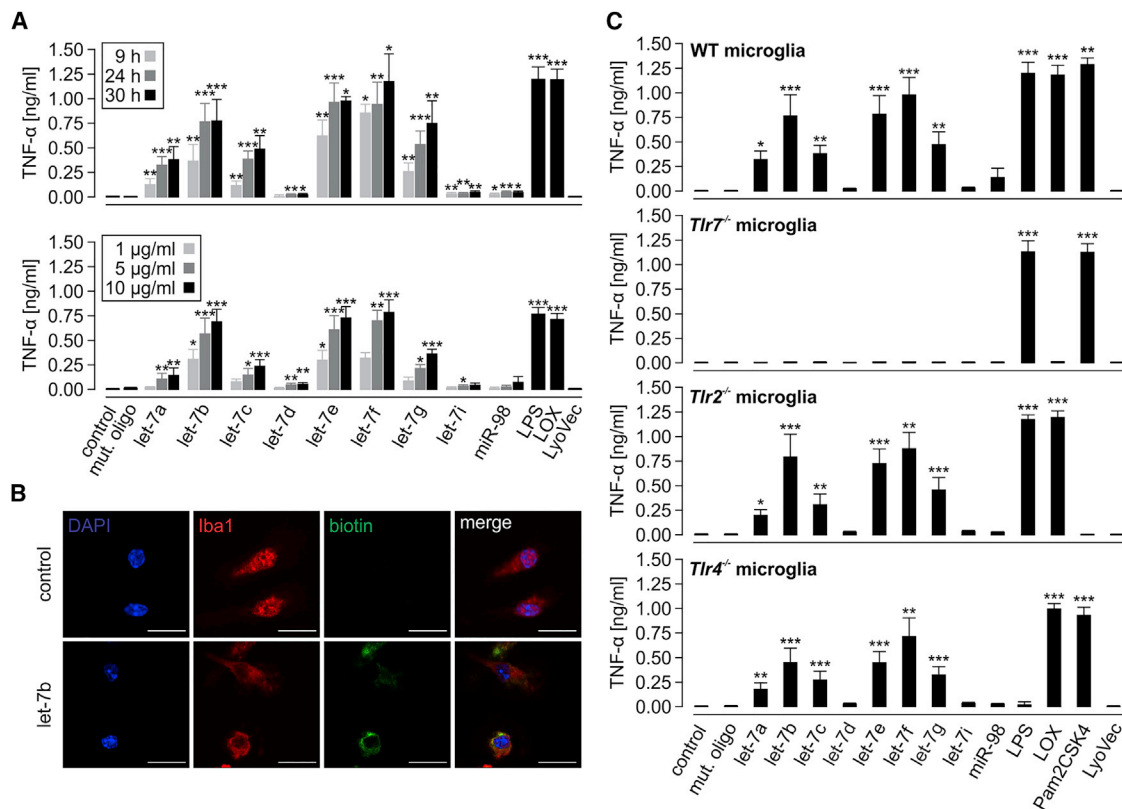
Figure 1. Extracellularly Delivered Different *let-7* miRNA Family Members Trigger TNF-α Release from Microglia Time- and Dose-Dependently via TLR7, but Not TLR2 or TLR4

(A) Primary neonatal microglia from wild-type (WT) mice were stimulated with 5 μg/mL of *let-7a-let-7i* or *miR-98* oligoribonucleotides for 9, 24, or 30 h (top) or with 1, 5, or 10 μg/mL of *let-7a-let-7i* or *miR-98* oligoribonucleotides for 24 h (bottom). TNF-α release was determined using ELISA. Lipopolysaccharide (LPS; 100 ng/mL) and loxoribine (LOX; 1 mM) were used as known TLR4 and TLR7 activators, respectively, while mutant oligoribonucleotide (mut. oligo; 5 μg/mL) and LyoVec served as negative controls. n = 5.

(B) Representative images of cultured neonatal microglia from WT mice incubated with 5 μg/mL biotinylated *let-7b* for 6 h. Cells were stained with Iba1 antibody and DAPI. Unstimulated microglia served as control. Scale bar, 30 μm.

(C) Primary neonatal microglia from WT, *Tlr7*$^{-/-}$, *Tlr2*$^{-/-}$, and *Tlr4*$^{-/-}$ mice were stimulated with 5 μg/mL *let-7a- let-7i* and *miR-98* for 24 h. TNF-α release was determined using ELISA. LPS (100 ng/mL), LOX (1 mM), and Pam2CSK4 (100 ng/mL) were used as positive controls for TLR4, TLR7, and TLR2 activation, respectively, while incubation with mut. oligo (5 μg/mL) and LyoVec served as negative controls. n = 5.

Data are represented as mean ± SEM. *p < 0.05, **p < 0.01, and ***p < 0.001 versus control (Kruskal-Wallis followed by Dunn's post hoc test).

See also Figure S1 and Table S1.

from bone marrow-derived macrophages stimulated with *let-7b*, *let-7e*, *let-7f*, and *let-7g* (Figure 2). In contrast to microglia, TNF-α release at 24 and 30 h was not different from TNF-α release at 9 h (Figure S2). *let-7d*, *let-7i*, and *miR-98* stimulation did not result in TNF-α production in macrophages (Figure 2). Taken together, extracellularly delivered *let-7* miRNAs differentially induce microglial activation through TLR7. The ability of microglia to respond to *let-7* miRNAs does not depend on their developmental stage, implying a functional role for extracellular *let-7* miRNAs in CNS diseases occurring at all ages. The precise local concentrations of extracellularly functional *let-7b* (or other members of the *let-7* miRNA family) in the brain parenchyma at the site of injury/pathology *in vivo* are not known. For this reason, the concentrations of *let-7* miRNAs used in the present study were based on our previous work on ssRNA-mediated neurodegeneration, in which we found that injured neurons, and potentially other

CNS cells, release *let-7b* into the extracellular space (Lehmann et al., 2012a, 2012b). Future work will be required to determine pathophysiological concentrations of *let-7* miRNAs in the brain.

Select *let-7* miRNAs Induce a Specific Pattern of Inflammatory Molecules Released from Microglia through TLR7

Although TNF-α is a well-studied cytokine released in response to TLR activation, additional cytokines and chemokines are also released from microglia. To determine the specific inflammatory response pattern induced by *let-7* miRNAs via TLR7, we used a multiplex immunoassay and analyzed the supernatants from neonatal WT and *Tlr7*$^{-/-}$ microglia incubated with 5 μg/mL of the respective *let-7* miRNA family member after 24 h. Mutant oligoribonucleotide and the TLR7 ligand LOX served as controls. IL-6, IL-10, IL-1β, GRO-α, MIP-2, and
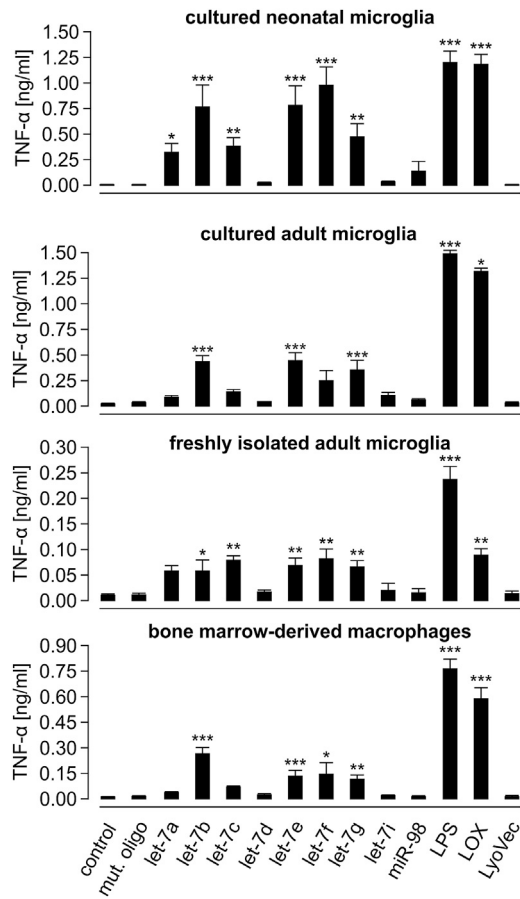
Figure 2. Neonatal and Adult Microglia, as Well as Bone Marrow-Derived Macrophages, Respond to Extracellularly Delivered *let-7* miRNAs

Primary cultured neonatal, adult cultured microglia, freshly isolated microglia, and primary bone marrow-derived macrophages from adult WT mice were stimulated with 5 μg/mL *let-7a-let-7i* or *miR-98* oligoribonucleotides, as indicated, for 24 h. TNF-α levels were determined using ELISA. LPS (100 ng/mL) and LOX (1 mM) were used as TLR4 and TLR7 ligands, respectively. Mut. oligo (5 μg/mL) and LyoVec served as negative controls. n = 4–6. Data are represented as mean ± SEM. *p < 0.05, **p < 0.01, and ***p < 0.001 versus control (Kruskal-Wallis followed by Dunn's post hoc test).
See also Figure S2.

RANTES were released from WT microglia after *let-7a*, *let-7b*, *let-7c*, *let-7e*, *let-7f*, and *let-7g* stimulation in a sequence-dependent fashion, while incubation with *let-7d*, *let-7i*, or *miR-98* did not result in much cytokine release (Figure 3A; Table S2). GM-CSF, IP-10, MCP-1, and MCP-3 were not increased after stimulation with any of the *let-7* miRNAs tested (Figure S3; Table S3). IL-6, IL-10, IL-1β, GRO-α, MIP-2, and RANTES induction required TLR7, as TLR7-deficient cells failed to respond to *let-7* miRNA (Figure 3A). MIP-1α and MIP-1β were released from microglia in response to all tested *let-7* miRNAs, but this response was not dependent on TLR7 (Figure S3). In summary, selected extracellularly delivered *let-7* miRNA family members induce a sequence-specific and TLR7-dependent inflammatory response with a distinct profile of cytokine release. Although
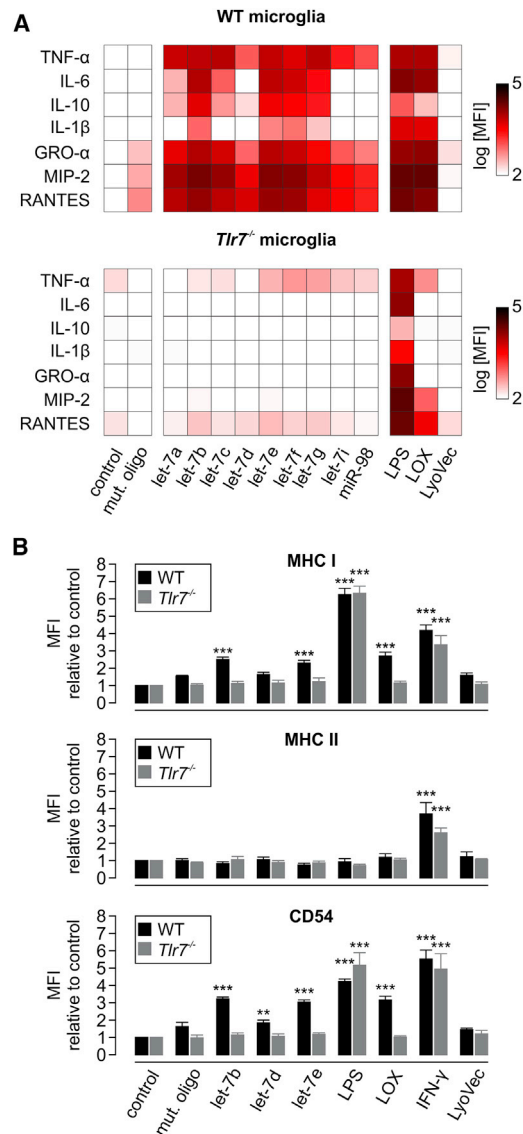

Figure 3. Characterization of the Microglial Inflammatory Response and Antigen-Presenting Marker Expression Induced by *let-7* miR-NAs through TLR7

(A) Multiplex immunoassay was performed to characterize the inflammatory response in WT (top) and *Tlr7*⁻/⁻ (bottom) microglia in response to *let-7b*, *let-7d*, and *let-7e* using the supernatants collected for TNF-α analysis in Figure 1. Data are shown in a heatmap representing cytokine release expressed in logarithmic of mean fluorescence intensity (MFI). LPS, LOX, and mut. oligo and LyoVec were used as positive and negative controls, respectively. n = 5. For p values yielded by Kruskal-Wallis test followed by Dunn's multiple comparison post hoc test, refer to Table S2.

(B) Primary neonatal microglia from WT and *Tlr7*⁻/⁻ mice were incubated with 5 μg/mL *let-7b*, *let-7d*, and *let-7e* for 24 h. MHC I, MHC II, and CD54 expression were analyzed using FACS. Marker expression is shown as mean fluorescent intensity (MFI) normalized to unstimulated control. LPS (100 ng/mL), LOX (1 mM), and IFN-γ (100 ng/mL) served as positive controls. Mut. oligo (5 μg/mL) and LyoVec served as negative controls. n = 4–10.

Data are represented as mean ± SEM. *p < 0.05, **p < 0.01, and ***p < 0.001 versus control (one-way ANOVA followed by Bonferroni post hoc test).
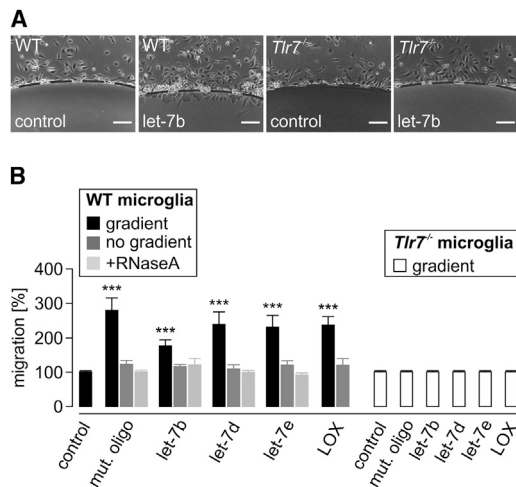See also Figures S3 and S4 and Table S3.

Figure 4. Small Oligoribonucleotides Including *let-7* miRNAs Induce Chemotaxis in Microglia via TLR7

Microglial migration in response to *let-7b*, *let-7d*, and *let-7e* oligoribonucleotides was analyzed by agarose spot assay.

(A) Images of *let-7b*-treated and control microglial cultures from WT and *Tlr7*$^{-/-}$ mice. Scale bar, 100 μm.

(B) *let-7b*, *let-7d*, or *let-7e* (5 μg/mL) was added either to the spot alone (gradient/black) or both to the spot and the culture medium (no gradient/dark gray) with (light gray) or without RNase A pre-incubation. Microglial migration in response to 5 μg/mL *let-7b*, *let-7d*, or *let-7e* was also analyzed in *Tlr7*$^{-/-}$ (white) microglia. PBS was used as negative control. Microglial migration was analyzed after 3 h of incubation. n = 8.

Data are represented as mean ± SEM. *p < 0.05, **p < 0.01, and ***p < 0.001 versus control (one-way ANOVA followed by Bonferroni post hoc test).

some of the inflammatory molecules, including TNF-α, IL-6, and IL-1β, have previously been reported as outputs of increased TLR7 signaling (Petes et al., 2017) and in the setting of glioma (Dzaye et al., 2016; Bowman et al., 2016; Zhu et al., 2012), the pattern of cytokines and chemokines determined in our study reflects the specific *let-7* miRNA family member used to stimulate microglia. Because *let-7* miRNAs differ only slightly within their GU-rich sequence motifs (see below), these data explain how individual miRNAs serving as signaling molecules may modify CNS inflammation in a sequence-dependent manner. In addition, our findings raise the possibility that specific combinations of inflammatory molecules may uniquely affect brain disease pathogenesis. For example, select *let-7* miRNA family members induce IL-6 release from microglia, which has been previously shown to promote the invasiveness of glioma cells (Zhang et al., 2012).

let-7b and *let-7e* Modulate the Expression of Antigen-Presenting Markers via TLR7

Microglia act as antigen-presenting cells in the CNS, regulating innate and adaptive immune responses. Major histocompatibility complex (MHC) class I is expressed by all nucleated cells and is responsible for the activation of CD8$^+$ T cells and natural killer cells, while MHC II is expressed by immune cells and activates CD4$^+$ T cells. CD54 (ICAM-1) is also important for antigen presentation (Werner et al., 1998; Zuckerman et al., 1998). Microglia from WT and *Tlr7*$^{-/-}$ mice were analyzed using FACS for MHC I,

MHC II, and CD54 expression following stimulation with 5 μg/mL *let-7b* and *let-7e*, which were observed to induce a potent cytokine response in microglia, and *let-7d*, which comparatively induced a weak cytokine response, for 24 h. LPS, loxoribine and IFN-γ were used as positive controls for TLR4 and TLR7 activation, as well as general microglial activation, respectively (Figure 3B; for FACS gating strategy and histogram plots, see Figure S4). Treatment with *let-7b* and *let-7e*, but not *let-7d*, increased MHC I, but not MHC II, expression. CD54 expression was increased in response to *let-7b* and *let-7e* and to a lesser extent to *let-7d* in microglia. *let-7*-miRNA-induced upregulation of MHC I and CD54 expression required TLR7, as *Tlr7*$^{-/-}$ microglia did not respond to the treatments (Figure 3B). In summary, select *let-7* miRNAs affected the expression of specific molecules crucial for antigen presentation in the CNS. MHC I and CD54 expression was dependent on TLR7. Both molecules are important for the communication between innate and adaptive immune cells. Specifically, MHC I is recognized by cytotoxic T cells, triggering an immediate immune response against a non-self-antigen, and natural killer cells, which directly kill antigen-presenting cells, such as virus-infected or tumor cells. Whether MHC I and CD54 expression in microglia in response to *let-7* miRNAs directly triggers T cell and natural killer cell activation remains unexplored at this stage and requires further investigation.

Select *let-7* miRNAs Induce Chemotaxis, but Not Motility, in Microglia through TLR7

In response to brain injury or pathology, microglia migrate to the afflicted sites, where they phagocytose pathogens, apoptotic cells, and cellular debris. We have previously shown that chemotaxis is controlled by TLR7 in microglia (Ifuku et al., 2016). As *let-7* miRNAs were found to serve as signaling activators of TLR7 in microglia, thereby inducing an inflammatory response, we investigated the *let-7* miRNAs' impact on microglial migration. To this end, microglia stimulated with *let-7b*, *let-7e*, and *let-7d* were analyzed using an agarose spot assay with a gradient to evaluate directed migration or without a gradient to test motility (Figures 4A and 4B). The *let-7* miRNAs as well as mutant oligoribonucleotides were added either to the spot alone or into both the spot and the medium. Cells that entered the spot within 3 h were quantified. PBS was used as negative control. *let-7b*, *let-7d*, and *let-7e*, but also the mutant oligoribonucleotide, increased microglial chemotaxis, but not motility, compared with control (Figure 4B), suggesting that small RNA molecules induce chemotaxis of microglia, independent of their sequence. Pre-treatment of the oligoribonucleotides with RNase A abolished migration, confirming the specificity of microglial migration induced by ssRNAs (Figure 4B). To determine whether TLR7 is involved in microglial migration induced by small oligoribonucleotides, we performed agarose spot assay with microglia from *Tlr7*$^{-/-}$ mice, using the same protocol previously used for WT microglia. TLR7-deficient microglia did not show increased migration when incubated with *let-7b*, *let-7d*, *let-7e*, or mutant oligoribonucleotides compared with control, implying that the migratory effect on microglia is dependent on TLR7 (Figures 4A and 4B). Taken together, incubation of microglia with *let-7b*, *let-7d*, and also *let-7e* led to increased migration. Our finding that a mutant control oligoribonucleotide lacking the
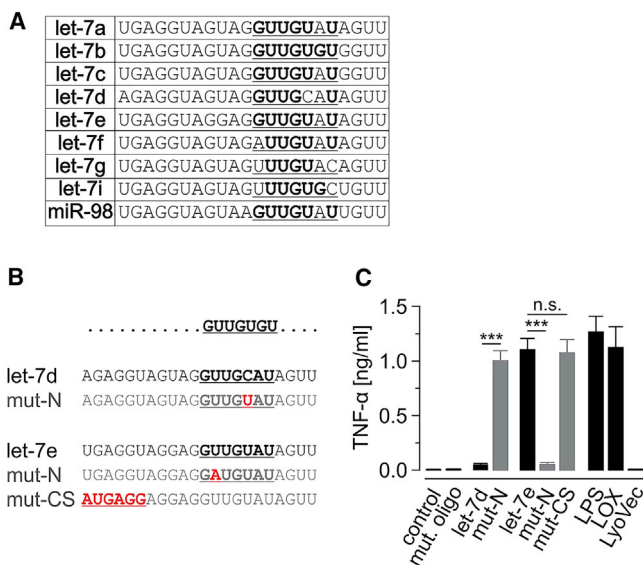
A

let-7a	UGAGGUAGUAG**GUUGUAU**AGUU
let-7b	UGAGGUAGUAG**GUUGUGU**GGUU
let-7c	UGAGGUAGUAG**GUUGUAU**GGUU
let-7d	AGAGGUAGUAG**GUUGCAU**AGUU
let-7e	UGAGGUAGGAG**GUUGUAU**AGUU
let-7f	UGAGGUAGUAG**AUUGUAU**AGUU
let-7g	UGAGGUAGUAG**UUUGUAC**AGUU
let-7i	UGAGGUAGUAGU**UUGUGC**UGUU
miR-98	UGAGGUAGUAA**GUUGUAU**UGUU

B

.........**GUUGUGU**....

let-7d AGAGGUAGUAG**GUUGCAU**AGUU
mut-N   AGAGGUAGUAG**GUUGU**AUAGUU (U in red)

let-7e UGAGGUAGGAG**GUUGUAU**AGUU
mut-N   UGAGGUAGGAG**GA**UGUAUAGUU (GA in red)
mut-CS **AUGAGG**AGGAGGUUGUAUAGUU (AUGAGG in red)

C

Figure 5. UUGU Is the Minimal Motif in *let-7* miRNAs Required for Activation of Microglial TLR7

(A) Sequences of *let-7* miRNA family members with indicated GU-rich TLR7 recognition motifs.

(B) Representation of *let-7d*'s and *let-7e*'s core motifs and corresponding mutations (red).

(C) Supernatants from WT microglia stimulated with 5 μg/mL of unmodified *let-7e* and *let-7d*, as well as with 5 μg/mL of the mutated oligoribonucleotides *let-7d*-mut-N, *let-7e*-mut-N, and *let-7*-mut-CS, for 24 h were analyzed by TNF-α ELISA. n = 3.

Data are represented as mean ± SEM. ***p < 0.001 mutated oligoribonucleotide versus respective naive oligoribonucleotide (one-way ANOVA followed by Bonferroni post hoc test).

GU-rich core motif also attracted microglia was unexpected and implies that, in contrast to the inflammatory response, microglia migration is modulated by small RNA in general but is not dependent on their sequence. Although we observed modulation of inflammatory response, antigen presentation, and migration by extracellularly delivered *let-7* miRNAs, we did not observe any effect on microglial phagocytosis (unpublished data).

The selective modulation of microglial functions suggests that *let-7*, and perhaps other miRNA species, elicit a specific reprogramming of microglia that promotes some, but not all, physiological processes important for brain homeostasis. Still, the findings reported herein so far raise several important points regarding microglia function in the brain. First, microglial activation following *let-7* exposure is a highly specific cellular response. It is not due to non-specific binding and/or the presence of contaminating factors. To this end, we used both a highly purified control mutant oligoribonucleotide, in which the GU content of the *let-7* core motif was modified, and oligoribonucleotides, in which single nucleotides of the *let-7* miRNA's sequence motifs were exchanged. Both control groups of oligoribonucleotides were handled and prepared identically to the respective *let-7* miRNA tested, making it unlikely that the microglial response to the *let-7* miRNA family was unspecific. TLR2- and TLR4-deficient but not TLR7-deficient microglia responded in a similar way to *let-7* miRNAs as WT microglia, excluding the possibility that

microglial activation after *let-7* miRNA incubation was due to the presence of endotoxin or lipoproteins. These responses occurred independent of microglia developmental stage (Scheffel et al., 2012), as neonatal and adult microglia behaved similarly. Finally, RNase treatment of *let-7* miRNAs abolished microglial migration, confirming the RNA nature of the agents tested.

The Sequence Motif UUGU Is Required for *let-7* miRNA-Induced Activation of TLR7 in Microglia

let-7 miRNA family members exhibit different capacities to activate microglia, reflecting sequence specificity. The *let-7* miRNA family is highly conserved between and within species, differing only in 1–4 nt among its members (Roush and Slack, 2008). As such, *let-7b* possesses a sequence that contains the established TLR7 recognition motif GUUGUGU within its 3' terminus (Diebold et al., 2004; Heil et al., 2004; Lehmann et al., 2012a). Other *let-7* miRNAs such as *let-7a*, *let-7c*, *let-7d*, *let-7e*, *let-7f*, *let-7g*, *let-7i*, and *miR-98* contain similar GU-rich motifs with minimal exchanges of nucleotides (Roush and Slack, 2008). To determine the minimal motif within *let-7* being necessary for microglial activation through TLR7, we used mutagenesis strategies, thereby analyzing the different *let-7* miRNA family members (Table S1) with regard to their sequence-dependent potential to activate microglia. We observed that other family members besides *let-7b*, which lack this GUUGUGU motif, also activate microglia in a TLR7-dependent fashion. Specifically, the core motifs of *let-7a*, *let-7c*, *let-7e*, *let-7f*, and *let-7g* do not contain the last guanine and/or uridine. In addition, *let-7f* and *let-7g* do not possess guanine in the first position of the motif, and *let-7d*, which does not activate TLR7, contains a cytosine instead of the third uridine (Figure 5A). As TLR7-dependent microglial activation was induced by *let-7e* but not *let-7d*, we hypothesized that the UUGU motif is responsible for microglial activation. To confirm this, we synthesized *let-7d* and *let-7e* mutant oligoribonucleotides: *let-7d*-mut-N (UUGC mutated to UUGU), *let-7e*-mut-N (UUGU mutated to AUGU), and *let-7e*-mut-CS (no mutation in the UUGU motif but upstream to this sequence) (Figure 5B). As expected, a point mutation in the *let-7d* core motif induced TLR7 activation and subsequent TNF-α release from microglia. In contrast, the point mutation in the *let-7e* core motif reduced TNF-α release. The mutation of six nucleotides at the 5' end of *let-7e*-mut-CS did not affect TNF-α levels compared with stimulation with the unmodified *let-7e* oligoribonucleotide, indicating that the presence of the UUGU core motif is sufficient for TLR7-dependent microglia activation (Figure 5C). In conclusion, these data imply that only the core sequence of four nucleotides, namely, UUGU, is required for *let-7* miRNA-induced activation of microglia through TLR7. These findings are in accordance with those of previous studies that identified the sequence UUGU as minimum motif required for TLR7/TLR8-mediated cytokine responses mediated by human peripheral blood mononuclear cells (Forsbach et al., 2008). This selectivity is important because it supports a model in which different *let-7* miRNA family members have unique roles in modulating microglia function. Our finding that the UUGU sequence is required as a minimum core motif for *let-7*-induced microglial activation is relevant to our overall understanding of the specificity of the interactions between an extracellular miRNA and its cognate receptor, especially in the setting of brain disease
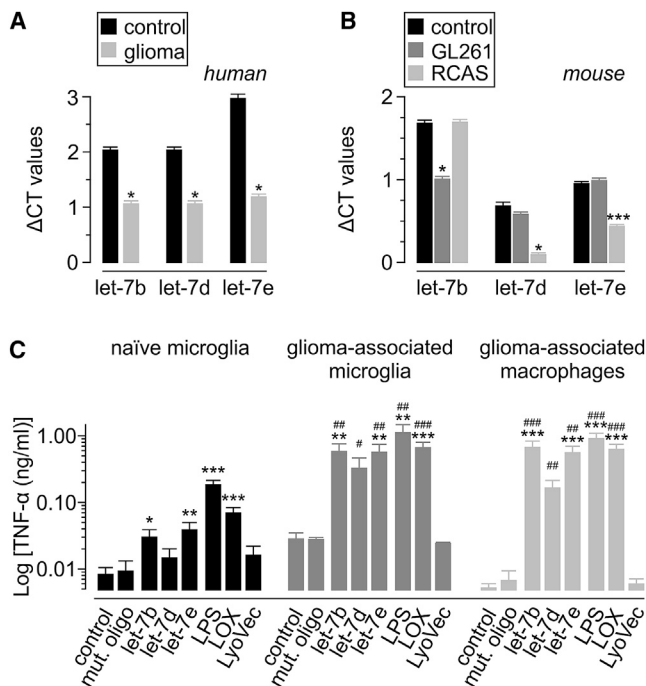
Figure 6. *let-7b* and *let-7e* Are Differentially Expressed in GBM and Act as Signaling Molecules on Glioma-Associated Microglia and Macrophages

(A and B) Relative *let-7b*, *let-7d*, and *let-7e* expression levels were assessed in (A) tumor tissue from GBM patients and control tissue (patients with epilepsy) and (B) tumor tissue from the murine glioma models GL261 or RCAS-hPDGFb and in healthy murine brain tissue. *miR-16* was used as housekeeping control. n = 5 for human tissue samples, and n = 5–8 for mouse tissue samples of both glioma models. Data are represented as mean ± SEM. Human data were analyzed using the Mann-Whitney U test. Mouse data were analyzed using one-way ANOVA followed by Dunnett's post hoc test. *p < 0.05, **p < 0.01, and ***p < 0.001 versus control.

(C) Freshly isolated naive microglia (black), GL261-derived glioma-associated microglia (dark gray), or glioma-associated macrophages (light gray) were stimulated with 5 μg/mL *let-7b*, *let-7d*, or *let-7e* for 24 h. LPS (100 ng/mL), LOX (1 mM), and mut. oligo (5 μg/mL) and LyoVec were used as positive and negative controls, respectively. TNF-α was detected using ELISA. n = 3–6.

Data are represented as logarithm of mean ± SEM. The Kruskal-Wallis test followed by Dunn's post hoc test was used within each group. *p < 0.05, **p < 0.01, and ***p < 0.001 versus respective control condition. The Mann-Whitney U test was performed comparing GAMs versus naive microglia. #p < 0.05, ##p < 0.01, and ###p < 0.001 versus naive microglia.

See also Figure S5.

pathogenesis in which different *let-7* molecules may be released. These findings provide potential new targets for therapeutic strategies, such as the development of inhibitor/agonist miRNAs as modulators of microglial activation in specific CNS disorders.

let-7 miRNAs Are Differentially Expressed in Glioma and Induce TNF-α Release from Glioma-Associated Microglia and Macrophages

On the basis of our previous studies on *let-7b* as a signaling molecule for neurons (Lehmann et al., 2012a), we suggest that CNS cells, including immune cells, release *let-7* miRNAs into the extracellular space, resulting in microglia activation. Whether

cellular *let-7* miRNAs passively leak into the extracellular space of the CNS or are actively secreted in their native state or enclosed in vesicles is unclear (Carlsbecker et al., 2010; Mittelbrunn et al., 2011). It has been recently shown that lung tumor cells release *miR-21* and *miR-29a* inside exosomes. These miRNAs are phagocytosed by macrophages and activate murine TLR7 and human TLR8 (Fabbri et al., 2012). Whether this mechanism plays a role in *let-7*-mediated microglial activation remains to be elucidated. Our results extend the physiological role of *let-7* miRNAs beyond their established role in regulation of gene expression to ligand-mediated activation of receptors in microglia. *let-7* miRNAs function as signaling molecules in the brain, where they modulate CNS pathology and contribute to injury, tumor growth, and immune responses. It is well established that microglia/brain macrophages are highly abundant in brain tumor tissue, where they promote glioma growth (Hambardzumyan et al., 2016). There are various cellular interactions between microglia/brain macrophages and glioma cells mediated by several signaling molecules, including osteopontin or versican (Hu et al., 2015; Szulzewsky et al., 2018). Furthermore, *let-7* miRNAs are differentially expressed in GBM and inhibit tumor growth by gene silencing (Degrauwe et al., 2016; Lee et al., 2011; Mao et al., 2013; Song et al., 2016; Wang et al., 2016). Building upon our results, demonstrating that extracellular *let-7* miRNAs function as signaling molecules for microglia and macrophages, we next sought to translate these findings to the setting of glioma. We comparatively assessed the expression levels of the *let-7* miRNA family members in brain tissue derived from human glioma resection and in experimental mouse glioma models. Tumor samples from GBM patients, as well as tissue from the syngeneic GL261 and the induced RCAS/TV-a system mouse glioma models, were compared with control cortex tissue from patients with epilepsy and samples from healthy murine brain, respectively, using TaqMan PCR (Figures 6A and 6B). In human GBM samples, *let-7b*, *let-7d*, and *let-7e* expression levels were lower compared with control (Figure 6A). In glioma tissue derived from the murine GL261 model, *let-7b* expression was lower (Figure 6B; for *let-7b* copy numbers, see Figure S5A), while the other *let-7* miRNAs showed no altered expression relative to control (Figure 6B). In glioma tissue from the murine RCAS model, *let-7d* and *let-7e* expression levels were lower compared with control (Figure 6B). *let-7g* and *miR-98* miRNA expression levels were lower in human GBM tissue, whereas in the RCAS model, tissue *let-7a*, *let-7c*, *let-7g*, and *miR-98* expression levels were lower relative to control (Figure S5B). In glioma tissue from the GL261 model, *let-7c* expression was lower, and *let-7g* expression was higher compared with control (Figure S5B). Expression levels of *miR-21* and *miR-210*, two established glioma-associated miRNAs (Malzkorn et al., 2010), were higher in human GBM and murine glioma tissue compared with control (Figure S5B). As noted above, we observed a TLR7-dependent induction of TNF-α from neonatal and adult microglia, as well as from macrophages, exposed to *let-7*. To determine how *let-7* miRNAs affect the function of glioma-associated microglia and macrophages (GAMs), GL261-associated microglia and invading macrophages, as well as freshly isolated naive microglia, were incubated with *let-7b*, *let-7d*, or *let-7e*, and TNF-α levels were measured in the respective supernatants using

ELISA. Microglia and macrophages both expressing GFP and only macrophages expressing RFP were isolated from *Cx3CR1-GFP x Ccr2-RFP* mice using FACS (Figure 6C). Compared with controls, GAMs released TNF-α in response to *let-7b* or *let-7e* exposure. The extent of these responses were similar to those seen following LPS and LOX treatment. Naive microglia responded to *let-7b* and *let-7e* with TNF-α release similar to that observed in postnatal and adult microglia (see Figure 2). Overall, the extent of TNF-α release from naive microglia in response to the *let-7* miRNAs tested was lower than those induced in GAMs (Figure 6C). *let-7d* did not induce TNF-α release relative to control. As observed for *let-7* miRNAs, levels of TNF-α induced by LPS and LOX in GAMs were also higher compared with those induced in naive microglia (Figure 6C). In summary, in human GBM and murine glioma, expression levels of a specific subset of *let-7* miRNAs including *let-7b* and *let-7e* were lower relative to control. These *let-7* miRNAs not only maintained their ability to activate microglia from glioma tissue but were even more potent inducers.

Extracellularly Delivered *let-7b* and *let-7e* Decrease GL261 Glioma Growth through TLR7 in Microglia *Ex Vivo*

To assess the functional impact of *let-7b*, *let-7e*, and *let-7d* as signaling molecules on glioma growth, we used organotypic mouse brain slice cultures injected with mCherry-labeled GL261 glioma cells. In this experimental paradigm, *let-7b*, *let-7d*, or *let-7e* oligoribonucleotides were constantly present in the culture medium. Four days after tumor injection, tumor volume using three-dimensional (3D) surface reconstruction was determined (Figure 7A). *let-7b* and *let-7e* treatment resulted in reduced tumor volume compared with untreated slices. In contrast, *let-7d* treatment had no effect on tumor growth (Figures 7A and 7B). To investigate whether *let-7* miRNA-mediated tumor reduction was dependent on TLR7, *Tlr7*$^{-/-}$ brain slices injected with mCherry-GL261 tumor cells were also treated with extracellularly delivered *let-7b*, *let-7d*, or *let-7e* and analyzed as above. Tumors from *Tlr7*$^{-/-}$ brain slices did not show any significant change in volume when treated with *let-7b*, *let-7d*, or *let-7e* relative to control (Figure 7B), indicating that TLR7 is required for the *let-7b*- and *let-7e*-mediated reduction of the tumor volume *ex vivo*. To assess whether microglia are required for *let-7* miRNA-mediated tumor reduction, organotypic brain slices from WT mice were treated with clodronate-loaded liposomes for 24 h, followed 48 h later by the injection of glioma cells. As described previously (Markovic et al., 2005), tumors in microglia-depleted slices were smaller relative to microglia-containing slices, and tumor growth was not affected following exposure to *let-7b*, *let-7d*, or *let-7e* relative to controls (Figure 7B), demonstrating that microglia account for tumor reduction induced by extracellular *let-7b* and *let-7e*.

To further investigate the effect of *let-7* as a microglia signaling activator on glioma growth, we performed immunohistochemical analysis of the organotypic brain slices implanted with GL261 cells, as described above. Here, we focused on *let-7b*, the most prominent member of the *let-7* miRNA family, which showed strong effects with respect to microglial activation and glioma growth inhibition. Glioma treated with extracellularly delivered *let-7b* revealed increased TUNEL-positive apoptosis

and caspase-3 activation (Figure 7C). These effects were not observed in brain slices incubated with *let-7d* (Figure 7C), which did not activate microglia and did not affect GL261 tumor growth. We detected reduced cell viability (Figure 7D) and increased TUNEL-positive apoptosis and caspase-3 activation (Figure 7E) in GL261 cells following exposure to microglia-conditioned medium treated with extracellularly delivered *let-7b*. Again, this effect was sequence dependent, as *let-7d* did not induce such effects (Figures 7D and 7E).

Although TLR7 is expressed in neurons and microglia, little or no TLR7 expression has been reported in astrocytes (Carpentier et al., 2005; Lehmann et al., 2012a; Olson and Miller, 2004). To validate these findings, we measured TLR7 expression in microglia and astrocytes isolated from postnatal day (P) 14- and 12-week-old mice, as well as in GL261 and RCAS glioma cells, using qRT-PCR (Figure S6). Microglia from both P14- and 12-week-old mice expressed high levels of TLR7, whereas neonatal astrocytes and adult astrocytes expressed no or only low levels of TLR7, respectively. In GL261- and RCAS-derived glioma cells, TLR7 expression was not detectable (Figure S6).

In summary, our results imply a functional role for *let-7* miRNAs as signaling molecules in glioma. Specific extracellularly delivered *let-7* miRNAs not only mediate the interaction between microglia and glioma cells but also selectively suppress mouse glioma growth through microglial TLR7 signaling. Although we detected *let-7b*-mediated caspase-3-positive apoptosis in both the GL261 glioma model and in GL261 cells *in vitro*, the identification of the exact molecular mechanism responsible for the glioma reduction induced by extracellular *let-7* miRNAs will require further investigation. It is tempting to speculate that select *let-7* miRNAs serving as signaling molecules specifically reprogrammed microglial cytokine release, migration, and antigen presentation in a fashion that may have affected tumor growth. Moreover, *let-7* miRNA family members act as chemoattractants for microglia and could increase microglia infiltration in glioma. In addition to the *let-7* miRNAs' impact on tumor growth as TLR7 signaling activators, in their function as gene regulators on a posttranscriptional level they may directly target oncogene expression. Indeed, *let-7* miRNAs have anti-tumorigenic effects in GBM cells by silencing stem cell programs, such as reducing RAS (Lee et al., 2011) or E2F2 (Song et al., 2016) expression. Thus, a greater understanding of the *let-7* miRNAs' role in both direct microglia signaling and posttranscriptional changes may reveal potential roles for them as new therapeutic targets for GBM patients (Gilles and Slack, 2018).

Conclusion

let-7 miRNAs in their unconventional form as signaling molecules differentially induce microglial activation mediated by TLR7 in a sequence-dependent fashion, thereby modulating diverse functions of these cells, including inflammatory responses, migration, and antigen presentation. Translating these findings to a CNS disease context, we found that select *let-7* miRNAs serving as signaling activators of microglia attenuate glioma growth. Future studies will be required to define the mechanisms underlying the
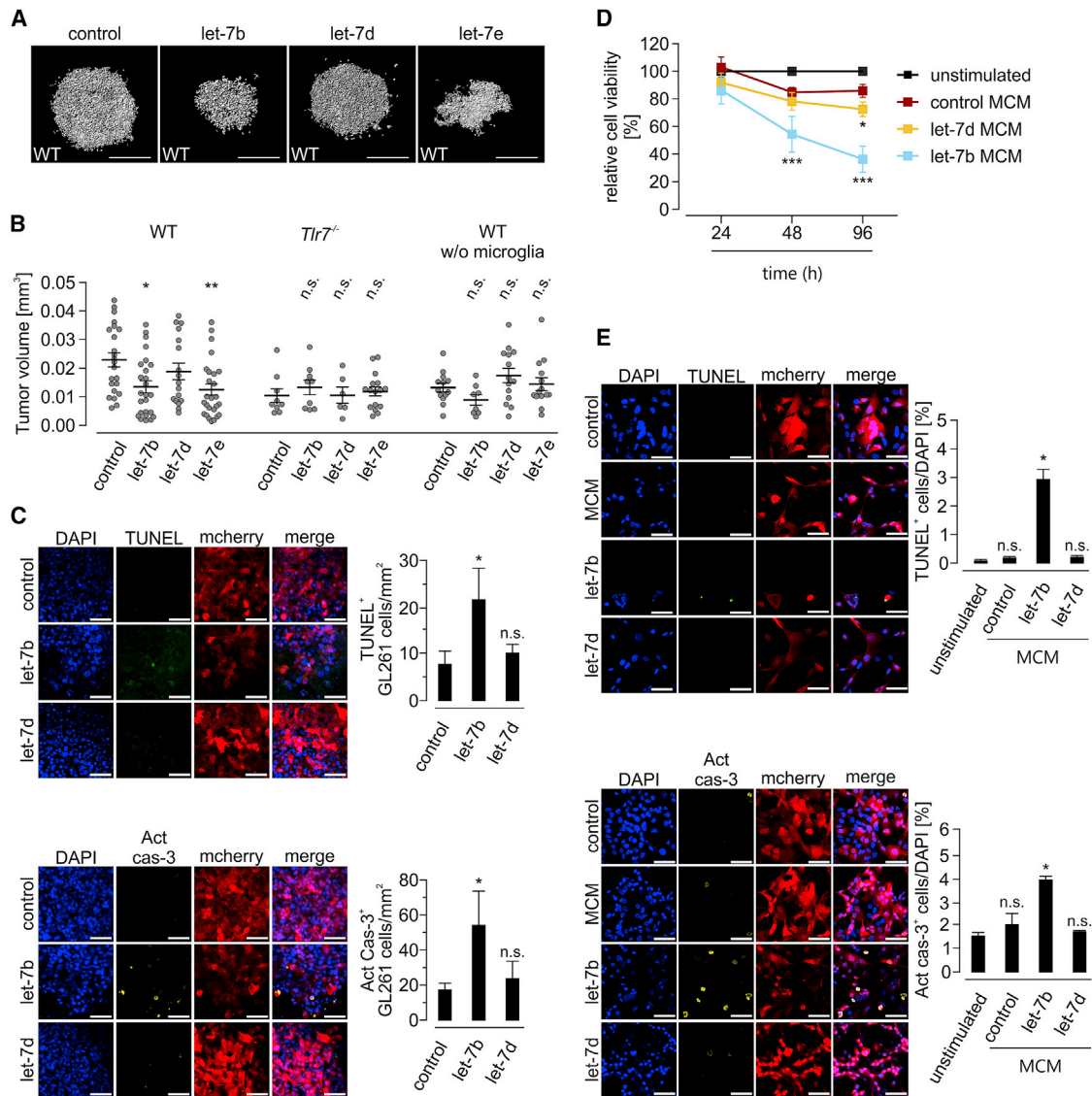
Figure 7. *let-7b* and *let-7e* Inhibit Glioma Growth through TLR7 and Microglia

(A) Three-dimensional surface reconstruction of glioma tumors in organotypic brain slices from WT mice incubated with *let-7b*, *let-7d*, or *let-7e* for 4 days post-tumor injection. Scale bar, 500 μm.

(B) Quantification of tumor volumes in WT, *Tlr7*$^{-/-}$, and microglia-depleted WT organotypic brain slices treated with 5 μg/mL *let-7b*, *let-7d*, or *let-7e*. Data are represented as mean ± SEM. Brain slices from n = 4–8 biological replicates. *p < 0.05, **p < 0.01, and ***p < 0.001 versus control (one-way ANOVA followed by Bonferroni post hoc test).

(C) Organotypic WT brain slices implanted with mCherry GL261 cells and incubated with *let-7b* or *let-7d* for 4 days were stained with TUNEL assay (upper image) and immunostained with activated caspase-3 antibody (lower image), as well as DAPI. Scale bar, 50 μm. Quantification of TUNEL-positive (upper graph) and activated caspase-3-positive (lower graph) cells. Data are represented as mean ± SEM. Brain slices from n = 4 biological replicates. *p < 0.05 versus control (one-way ANOVA followed by Bonferroni post hoc test).

(D) Viability of GL261 tumor cells treated with *let-7b*-, *let-7d*-stimulated microglial conditioned medium (MCM) or control MCM for 24, 48, and 96 h. Data are represented as mean ± SEM; n = 4. *p < 0.05 and ***p < 0.001 versus control (one-way ANOVA followed by Bonferroni post hoc test).

(E) GL261 cells were treated with *let-7b*-, *let-7d*- MCM or control MCM for 48 h. Cells were stained with TUNEL assay (upper image) and immunostained with activated caspase-3 antibody (lower image). Scale bar, 50 μm. Quantification of TUNEL-positive (upper graph) and activated caspase-3-positive (lower graph) cells. Unstimulated GL261 cells and control MCM were used as controls. Data are represented as mean ± SEM; n = 6 or 7. *p < 0.05 versus control (one-way ANOVA followed by Bonferroni post hoc test). n.s., not significant.

See also Figure S6.

let-7 miRNAs' regulatory roles as signaling molecules in microglia in health and disease.

STAR★METHODS

Detailed methods are provided in the online version of this paper and include the following:

- KEY RESOURCES TABLE
- LEAD CONTACT AND MATERIALS AVAILABILITY
- EXPERIMENTAL MODEL AND SUBJECT DETAILS
  - ○ Animals
  - ○ Human Biopsies
  - ○ Cell Lines
  - ○ Primary Cell Cultures
- METHOD DETAILS
  - ○ Isolation of Fresh Naive Adult Microglia and GAMs for Functional Assays
  - ○ let-7 miRNA Stimulation and TNF-α Enzyme-Linked Immunosorbent Assay
  - ○ Multiplex Immune Assay
  - ○ Agarose Spot Assay
  - ○ Flow Cytometry Analysis
  - ○ Tumor Injection *In Vivo*
  - ○ Total RNA Extraction and Quantitative RT-PCR
  - ○ Analysis of Cell Viability and Apoptosis in GL261 Cells
  - ○ Organotypic Brain Slice Cultures
  - ○ Tumor Cell Injection into Brain Slices and let-7 miRNA Treatment
  - ○ Depletion of Microglia
  - ○ Immunofluorescence, Confocal Microscopy, and Tumor 3D Reconstruction
- QUANTIFICATION AND STATISTICAL ANALYSIS
- DATA AND CODE AVAILABILITY

SUPPLEMENTAL INFORMATION

Supplemental Information can be found online at https://doi.org/10.1016/j.celrep.2019.11.029.

AUTHOR CONTRIBUTIONS

H.K. and S.L. conceptualized and supervised the study. H.K., S.L., A.B., and D.H.G. wrote the manuscript with input from all other authors. A.B., A.I., A.G.N., C.K., D.B., D.G., D.H.G., E.O., I.E.E., M.S., O.D., S.A.W., and Y.H. carried out the experiments and analyzed and/or discussed data. C.F., D.M., R.A.D., and U.C.S. provided the human biopsies.

DECLARATION OF INTERESTS

The authors declare no competing interests.

REFERENCES

Bartel, D.P. (2004). MicroRNAs: genomics, biogenesis, mechanism, and function. Cell *116*, 281–297.

Bowman, R.L., Klemm, F., Akkari, L., Pyonteck, S.M., Sevenich, L., Quail, D.F., Dhara, S., Simpson, K., Gardner, E.E., Iacobuzio-Donahue, C.A., et al. (2016). Macrophage ontogeny underlies differences in tumor-specific education in brain malignancies. Cell Rep. *17*, 2445–2459.

Carlsbecker, A., Lee, J.Y., Roberts, C.J., Dettmer, J., Lehesranta, S., Zhou, J., Lindgren, O., Moreno-Risueno, M.A., Vatén, A., Thitamadee, S., et al. (2010). Cell signalling by microRNA165/6 directs gene dose-dependent root cell fate. Nature *465*, 316–321.

Carpentier, P.A., Begolka, W.S., Olson, J.K., Elhofy, A., Karpus, W.J., and Miller, S.D. (2005). Differential activation of astrocytes by innate and adaptive immune stimuli. Glia *49*, 360–374.

Degrauwe, N., Schlumpf, T.B., Janiszewska, M., Martin, P., Cauderay, A., Provero, P., Riggi, N., Suvà, M.L., Paro, R., and Stamenkovic, I. (2016). The RNA binding protein IMP2 preserves glioblastoma stem cells by preventing let-7 target gene silencing. Cell Rep. *15*, 1634–1647.

Diebold, S.S., Kaisho, T., Hemmi, H., Akira, S., and Reis e Sousa, C. (2004). Innate antiviral responses by means of TLR7-mediated recognition of single-stranded RNA. Science *303*, 1529–1531.

Dzaye, O., Hu, F., Derkow, K., Haage, V., Euskirchen, P., Harms, C., Lehnardt, S., Synowitz, M., Wolf, S.A., and Kettenmann, H. (2016). Glioma stem cells but not bulk glioma cells upregulate IL-6 secretion in microglia/brain macrophages via Toll-like receptor 4 signaling. J. Neuropathol. Exp. Neurol. *75*, 429–440.

Fabbri, M., Paone, A., Calore, F., Galli, R., Gaudio, E., Santhanam, R., Lovat, F., Fadda, P., Mao, C., Nuovo, G.J., et al. (2012). MicroRNAs bind to Toll-like receptors to induce prometastatic inflammatory response. Proc. Natl. Acad. Sci. U S A *109*, E2110–E2116.

Feng, Y., Zou, L., Yan, D., Chen, H., Xu, G., Jian, W., Cui, P., and Chao, W. (2017). Extracellular microRNAs induce potent innate immune responses via TLR7/MyD88-dependent mechanisms. J. Immunol. *199*, 2106–2117.

Forsbach, A., Nemorin, J.G., Montino, C., Müller, C., Samulowitz, U., Vicari, A.P., Jurk, M., Mutwiri, G.K., Krieg, A.M., Lipford, G.B., and Vollmer, J. (2008). Identification of RNA sequence motifs stimulating sequence-specific TLR8-dependent immune responses. J. Immunol. *180*, 3729–3738.

Gilles, M.E., and Slack, F.J. (2018). Let-7 microRNA as a potential therapeutic target with implications for immunotherapy. Expert Opin. Ther. Targets *22*, 929–939.

Haage, V., Elmadany, N., Roll, L., Faissner, A., Gutmann, D.H., Semtner, M., and Kettenmann, H. (2019). Tenascin C regulates multiple microglial functions involving TLR4 signaling and HDAC1. Brain. Behav. Immun. *81*, 470–483.

Hambardzumyan, D., Amankulor, N.M., Helmy, K.Y., Becher, O.J., and Holland, E.C. (2009). Modeling Adult Gliomas using RCAS/t-va Technology. Transl. Oncol. *2*, 89–95.

Hambardzumyan, D., Gutmann, D.H., and Kettenmann, H. (2016). The role of microglia and macrophages in glioma maintenance and progression. Nat. Neurosci. *19*, 20–27.

He, S., Chu, J., Wu, L.C., Mao, H., Peng, Y., Alvarez-Breckenridge, C.A., Hughes, T., Wei, M., Zhang, J., Yuan, S., et al. (2013). MicroRNAs activate natural killer cells through Toll-like receptor signaling. Blood *121*, 4663–4671.

Heil, F., Hemmi, H., Hochrein, H., Ampenberger, F., Kirschning, C., Akira, S., Lipford, G., Wagner, H., and Bauer, S. (2004). Species-specific recognition of single-stranded RNA via toll-like receptor 7 and 8. Science *303*, 1526–1529.

Hemmi, H., Kaisho, T., Takeuchi, O., Sato, S., Sanjo, H., Hoshino, K., Horiuchi, T., Tomizawa, H., Takeda, K., and Akira, S. (2002). Small anti-viral compounds activate immune cells via the TLR7 MyD88-dependent signaling pathway. Nat. Immunol. *3*, 196–200.

Hoshino, K., Takeuchi, O., Kawai, T., Sanjo, H., Ogawa, T., Takeda, Y., Takeda, K., and Akira, S. (1999). Cutting edge: Toll-like receptor 4 (TLR4)-deficient mice are hyporesponsive to lipopolysaccharide: evidence for TLR4 as Lps gene product. J. Immunol. *162*, 3749–3752.

Hu, F., Dzaye, O., Hahn, A., Yu, Y., Scavetta, R.J., Dittmar, G., Kaczmarek, A.K., Dunning, K.R., Ricciardelli, C., Rinnenthal, J.L., et al. (2015). Glioma-derived versican promotes tumor expansion via glioma-associated micro-glial/macrophages Toll-like receptor 2 signaling. Neuro Oncol. *17*, 200–210.

Ifuku, M., Buonfiglioli, A., Jordan, P., Lehnardt, S., and Kettenmann, H. (2016). TLR2 controls random motility, while TLR7 regulates chemotaxis of microglial cells via distinct pathways. Brain Behav. Immun. *58*, 338–347.

Kawai, T., and Akira, S. (2006). TLR signaling. Cell Death Differ. *13*, 816–825.

Kettenmann, H., Hanisch, U.K., Noda, M., and Verkhratsky, A. (2011). Physiology of microglia. Physiol. Rev. *91*, 461–553.

Lee, S.T., Chu, K., Oh, H.J., Im, W.S., Lim, J.Y., Kim, S.K., Park, C.K., Jung, K.H., Lee, S.K., Kim, M., and Roh, J.K. (2011). Let-7 microRNA inhibits the proliferation of human glioblastoma cells. J. Neurooncol. *102*, 19–24.

Lee, H., Han, S., Kwon, C.S., and Lee, D. (2016). Biogenesis and regulation of the let-7 miRNAs and their functional implications. Protein Cell *7*, 100–113.

Lehmann, S.M., Krüger, C., Park, B., Derkow, K., Rosenberger, K., Baumgart, J., Trimbuch, T., Eom, G., Hinz, M., Kaul, D., et al. (2012a). An unconventional role for miRNA: let-7 activates Toll-like receptor 7 and causes neurodegeneration. Nat. Neurosci. *15*, 827–835.

Lehmann, S.M., Rosenberger, K., Kruger, C., Habbel, P., Derkow, K., Kaul, D., Rybak, A., Brandt, C., Schott, E., Wulczyn, F.G., et al. (2012b). Extracellularly delivered single-stranded viral RNA causes neurodegeneration dependent on TLR7. J. Immunol. *189*, 1448–1458.

Louis, D.N., Perry, A., Reifenberger, G., von Deimling, A., Figarella-Branger, D., Cavenee, W.K., Ohgaki, H., Wiestler, O.D., Kleihues, P., and Ellison, D.W. (2016). The 2016 World Health Organization classification of tumors of the central nervous system: a summary. Acta Neuropathol. *131*, 803–820.

Malzkorn, B., Wolter, M., Liesenberg, F., Grzendowski, M., Stühler, K., Meyer, H.E., and Reifenberger, G. (2010). Identification and functional characterization of microRNAs involved in the malignant progression of gliomas. Brain Pathol. *20*, 539–550.

Manzanero, S. (2012). Generation of mouse bone marrow-derived macrophages. Methods Mol. Biol. *844*, 177–181.

Mao, X.G., Hütt-Cabezas, M., Orr, B.A., Weingart, M., Taylor, I., Rajan, A.K., Odia, Y., Kahlert, U., Maciaczyk, J., Nikkhah, G., et al. (2013). LIN28A facilitates the transformation of human neural stem cells and promotes glioblastoma tumorigenesis through a pro-invasive genetic program. Oncotarget *4*, 1050–1064.

Markovic, D.S., Glass, R., Synowitz, M., Rooijen, Nv., and Kettenmann, H. (2005). Microglia stimulate the invasiveness of glioma cells by increasing the activity of metalloprotease-2. J. Neuropathol. Exp. Neurol. *64*, 754–762.

Mittelbrunn, M., Gutiérrez-Vázquez, C., Villarroya-Beltri, C., González, S., Sánchez-Cabo, F., González, M.A., Bernad, A., and Sánchez-Madrid, F. (2011). Unidirectional transfer of microRNA-loaded exosomes from T cells to antigen-presenting cells. Nat. Commun. *2*, 282.

Napoli, I., and Neumann, H. (2009). Microglial clearance function in health and disease. Neuroscience *158*, 1030–1038.

Olson, J.K., and Miller, S.D. (2004). Microglia initiate central nervous system innate and adaptive immune responses through multiple TLRs. J. Immunol. *173*, 3916–3924.

Pannell, M., Meier, M.A., Szulzewsky, F., Matyash, V., Endres, M., Kronenberg, G., Prinz, V., Waiczies, S., Wolf, S.A., and Kettenmann, H. (2016). The subpopulation of microglia expressing functional muscarinic acetylcholine receptors expands in stroke and Alzheimer's disease. Brain Struct. Funct. *221*, 1157–1172.

Pasquinelli, A.E., Reinhart, B.J., Slack, F., Martindale, M.Q., Kuroda, M.I., Maller, B., Hayward, D.C., Ball, E.E., Degnan, B., Müller, P., et al. (2000). Conservation of the sequence and temporal expression of let-7 heterochronic regulatory RNA. Nature *408*, 86–89.

Pena, J.T., Sohn-Lee, C., Rouhanifard, S.H., Ludwig, J., Hafner, M., Mihailovic, A., Lim, C., Holoch, D., Berninger, P., Zavolan, M., and Tuschl, T. (2009). miRNA in situ hybridization in formaldehyde and EDC-fixed tissues. Nat. Methods *6*, 139–141.

Petes, C., Odoardi, N., and Gee, K. (2017). The Toll for trafficking: Toll-like receptor 7 delivery to the endosome. Front. Immunol. *8*, 1075.

Prinz, M., Kann, O., Draheim, H.J., Schumann, R.R., Kettenmann, H., Weber, J.R., and Hanisch, U.K. (1999). Microglial activation by components of gram-positive and -negative bacteria: distinct and common routes to the induction of ion channels and cytokines. J. Neuropathol. Exp. Neurol. *58*, 1078–1089.

Rajbhandari, L., Tegenge, M.A., Shrestha, S., Ganesh Kumar, N., Malik, A., Mithal, A., Hosmane, S., and Venkatesan, A. (2014). Toll-like receptor 4 deficiency impairs microglial phagocytosis of degenerating axons. Glia *62*, 1982–1991.

Ramirez-Ortiz, Z.G., Prasad, A., Griffith, J.W., Pendegraft III, W.F., Cowley, G.S., Root, D.E., Tai, M., Luster, A.D., El Khoury, J., Hacohen, N., et al. (2015). The receptor TREML4 amplifies TLR7-mediated signaling during antiviral responses and autoimmunity. Nat. Immunol. *16*, 495–504.

Reinhart, B.J., Slack, F.J., Basson, M., Pasquinelli, A.E., Bettinger, J.C., Rougvie, A.E., Horvitz, H.R., and Ruvkun, G. (2000). The 21-nucleotide let-7 RNA regulates developmental timing in Caenorhabditis elegans. Nature *403*, 901–906.

Roush, S., and Slack, F.J. (2008). The let-7 family of microRNAs. Trends Cell Biol. *18*, 505–516.

Saederup, N., Cardona, A.E., Croft, K., Mizutani, M., Cotleur, A.C., Tsou, C.L., Ransohoff, R.M., and Charo, I.F. (2010). Selective chemokine receptor usage by central nervous system myeloid cells in CCR2-red fluorescent protein knock-in mice. PLoS One *5*, e13693.

Sasmono, R.T., Oceandy, D., Pollard, J.W., Tong, W., Pavli, P., Wainwright, B.J., Ostrowski, M.C., Himes, S.R., and Hume, D.A. (2003). A macrophage colony-stimulating factor receptor-green fluorescent protein transgene is expressed throughout the mononuclear phagocyte system of the mouse. Blood *101*, 1155–1163.

Scheffel, J., Regen, T., Van Rossum, D., Seifert, S., Ribes, S., Nau, R., Parsa, R., Harris, R.A., Boddeke, H.W., Chuang, H.N., et al. (2012). Toll-like receptor activation reveals developmental reorganization and unmasks responder subsets of microglia. Glia *60*, 1930–1943.

Song, H., Zhang, Y., Liu, N., Zhang, D., Wan, C., Zhao, S., Kong, Y., and Yuan, L. (2016). Let-7b inhibits the malignant behavior of glioma cells and glioma stem-like cells via downregulation of E2F2. J. Physiol. Biochem. *72*, 733–744.

Stupp, R., Mason, W.P., van den Bent, M.J., Weller, M., Fisher, B., Taphoorn, M.J., Belanger, K., Brandes, A.A., Marosi, C., Bogdahn, U., et al.; European Organisation for Research and Treatment of Cancer Brain Tumor and Radiotherapy Groups; National Cancer Institute of Canada Clinical Trials Group (2005). Radiotherapy plus concomitant and adjuvant temozolomide for glioblastoma. N. Engl. J. Med. *352*, 987–996.

Szulzewsky, F., Pelz, A., Feng, X., Synowitz, M., Markovic, D., Langmann, T., Holtman, I.R., Wang, X., Eggen, B.J., Boddeke, H.W., et al. (2015). Glioma-associated microglia/macrophages display an expression profile different from M1 and M2 polarization and highly express Gpnmb and Spp1. PLoS ONE *10*, e0116644.

Szulzewsky, F., Schwendinger, N., Güneykaya, D., Cimino, P.J., Hambardzumyan, D., Synowitz, M., Holland, E.C., and Kettenmann, H. (2018). Loss of host-derived osteopontin creates a glioblastoma-promoting microenvironment. Neuro Oncol. *20*, 355–366.

Takeuchi, O., Hoshino, K., Kawai, T., Sanjo, H., Takada, H., Ogawa, T., Takeda, K., and Akira, S. (1999). Differential roles of TLR2 and TLR4 in

recognition of gram-negative and gram-positive bacterial cell wall components. Immunity *11*, 443–451.

Tang, D., Kang, R., Coyne, C.B., Zeh, H.J., and Lotze, M.T. (2012). PAMPs and DAMPs: signal 0s that spur autophagy and immunity. Immunol. Rev. *249*, 158–175.

Vinnakota, K., Hu, F., Ku, M.C., Georgieva, P.B., Szulzewsky, F., Pohlmann, A., Waiczies, S., Waiczies, H., Niendorf, T., Lehnardt, S., et al. (2013). Toll-like receptor 2 mediates microglia/brain macrophage MT1-MMP expression and glioma expansion. Neuro-oncol. *15*, 1457–1468.

Wang, Z., Lin, S., Zhang, J., Xu, Z., Xiang, Y., Yao, H., Ge, L., Xie, D., Kung, H.F., Lu, G., et al. (2016). Loss of MYC and E-box3 binding contributes to defective MYC-mediated transcriptional suppression of human MC-let-7a-1∼let-7d in glioblastoma. Oncotarget *7*, 56266–56278.

Werner, A., Kloss, C.U., Walter, J., Kreutzberg, G.W., and Raivich, G. (1998). Intercellular adhesion molecule-1 (ICAM-1) in the mouse facial motor nucleus after axonal injury and during regeneration. J. Neurocytol. *27*, 219–232.

Wiggins, H., and Rappoport, J. (2010). An agarose spot assay for chemotactic invasion. Biotechniques *48*, 121–124.

Wlodarczyk, A., Løbner, M., Cédile, O., and Owens, T. (2014). Comparison of microglia and infiltrating CD11c^{+} cells as antigen presenting cells for T cell proliferation and cytokine response. J. Neuroinflammation *11*, 57.

Zhang, J., Sarkar, S., Cua, R., Zhou, Y., Hader, W., and Yong, V.W. (2012). A dialog between glioma and microglia that promotes tumor invasiveness through the CCL2/CCR2/interleukin-6 axis. Carcinogenesis *33*, 312–319.

Zhu, V.F., Yang, J., Lebrun, D.G., and Li, M. (2012). Understanding the role of cytokines in glioblastoma multiforme pathogenesis. Cancer Lett. *316*, 139–150.

Zuckerman, S.H., Gustin, J., and Evans, G.F. (1998). Expression of CD54 (intercellular adhesion molecule-1) and the beta 1 integrin CD29 is modulated by a cyclic AMP dependent pathway in activated primary rat microglial cultures. Inflammation *22*, 95–106.

STAR★METHODS

KEY RESOURCES TABLE

REAGENT or RESOURCE	SOURCE	IDENTIFIER
Antibodies		
goat anti-Iba1	abcam	cat# ab5076; RRID: AB_2224402
Alexa Fluor 647 donkey anti-goat	Dianova	cat# 705-605-147; RRID: AB_2340437
DAPI	Dianova	cat# 32670; RRID: AB_2173853
CD45- eflour 450	eBioscience	cat# 48-0451-82; RRID: AB_1518806
CD11b- PE Cy7	eBioscience	cat# 25-0112-82; RRID: AB_469588
CD11b Monoclonal Antibody (M1/70), Alexa Fluor 700	eBioscience	cat# 56-0112-82; RRID: AB_657585
Anti-Mouse MHCI (H-2Kd/H-2Dd) FITC	eBioscience	cat# 11-5998-81; RRID: AB_465357
MHC Class II (I-A/I-E), (M5/114.15.2), APC-eFluor 780,	eBioscience	cat# 47-5321-82; RRID: AB_1548783
CD54 (ICAM-1), (YN1/1.7.4), FITC	eBioscience	cat# 11-0541-81; RRID: AB_465093
Avidin, NeutrAvidin, FITC conjugate	Thermo Fisher Scientific	cat# A2662; RRID:AB_2814980
Donkey IgG anti-Rabbit IgG (H+L) - Alexa Fluor 647	Dianova	Cat# 711-605-152; RRID:AB_ 2340625
Cleaved Caspase-3 (Asp175) Antibody	Cell signaling Technology	cat# 9661; RRID: AB_2341188
Bacterial and Virus Strains		
pRRL.PPT.MP.mcherry	AG Uckert	N/A
Biological Samples		
Human cortical tissue from epileptic surgery	Department of Neurosurgery, Charité-Universitätsmedizin Berlin	https://neurochirurgie.charite.de/en/
Glioblastoma patient-resected brain tissue	Department of Neurosurgery, Helios Clinic Buch	https://www.helios-gesundheit.de/kliniken/berlin-buch/unser-angebot/unsere-fachbereiche/neurochirurgie-und-wirbelsaeulentherapie/
	Department of Neurosurgery, University Medical Center Schleswig-Holstein	https://www.uksh.de/neurochirurgie-kiel/
Chemicals, Peptides, and Recombinant Proteins		
LyoVec^{TM} complexer	Invivogen	https://www.invivogen.com
LPS from *E. coli*, Serotype R515	Enzo Life Sciences	cat# ALX-581-007-L002
Loxoribine	Invivogen	cat# tlrl-lox
Pam2CSK4	Invivogen	cat# tlrl-pm2s-1
murine recombinant M-CSF	Peprotech	cat# 315-02
RNase A, DNase and protease-free	Thermo Fisher Scientific	cat# EN0531
Aqua-Poly/Mount	Polysciences	cat# 18606-5
Critical Commercial Assays		
*mir*Vana PARIS RNA and Native Protein Purification Kit	Thermo Fisher Scientific	*cat# AM1556*
TaqMan MicroRNA assays: hsa-let-7a, hsa-let-7b, hsa-let-7c, hsa-let-7d, hsa-let-7e, hsa-let-7f, hsa-let-7i, hsa-miR-98, hsa-miR-21, hsa-miR-210, hsa-miR-16	Thermo Fisher Scientific	*cat# 4427975*
TaqMan MicroRNA Reverse Transcription Kit	Thermo Fisher Scientific	*cat# 4366596*
TaqMan^{TM} universal Master Mix II no UNG	Thermo Fisher Scientific	*cat# 4440040*
Mouse TNF alpha ELISA Ready-SET-Go! Kit	Invitrogen	cat# 88-7324-88
ProcartaPlex Mix&Match Mouse 5-plex	Thermo Fisher Scientific	https://www.thermofisher.com/us/en/home/life-science/antibodies/immunoassays/procartaplex-assays-luminex/procartaplex-immunoassays/procartaplex-custom-panels.html

Continued

REAGENT or RESOURCE	SOURCE	IDENTIFIER
Chemokine 9-Plex Mouse ProcartaPlex	Thermo Fisher Scientific	*EPX090-20821-901*
Adult Brain Dissociation Kit	Miltenyi Biotech	cat# 130-107-677
Cell counting Kit-8 (CCK-8)	Tebu-bio	cat# CK04-05
In Situ Cell Death Detection Kit, Fluorescein	Roche	cat# 11684795910
ApopTag® Plus Fluorescein *In Situ* Apoptosis Detection Kit	Merck	cat# S7111
Experimental Models: Cell Lines		
Glioma 261 (GL261)	NCI	DTP, DCTC Tumor Repository, Frederick National Laboratory for Cancer Research, Frederick, Maryland
Experimental Models: Organisms/Strains		
Mouse: C57BL/6NCrl	Charles River Laboratories	N/A
Mouse: Tlr7$^{-/-}$	Hemmi et al., 2002	https://idp.nature.com/authorize?response_type=cookie&client_id=grover&redirect_uri=https%3A%2F%2Fwww.nature.com%2Farticles%2Fni758
Mouse: Tlr2$^{-/-}$	Takeuchi et al., 1999	https://www.sciencedirect.com/science/article/pii/S1074761300801193?via%3Dihub
Mouse: Tlr4$^{-/-}$	Hoshino et al., 1999	https://www.jimmunol.org/content/162/7/3749.long
Mouse: Cx3cr1$^{GFP/+}$ x Ccr2$^{RFP/+}$	Saederup et al., 2010	https://www.ncbi.nlm.nih.gov/pmc/articles/PMC2965160/
Mouse: Cfs1r-EGFP (Macgreen)	Sasmono et al., 2003	https://ashpublications.org/blood/article-lookup/doi/10.1182/blood-2002-02-0569
Mouse: *Nestin-tv-a;Ink4a-Arf*$^{-/-}$;*Pten*$^{fl/fl}$	Hambardzumyan et al., 2009	https://www.ncbi.nlm.nih.gov/pmc/articles/PMC2670576/
Oligonucleotides		
let-7a. 5′- UGAGGUAGUAGGUUGUAUAGUU −3′	Integrated DNA Technology	http://www.idtdna.com/pages
let-7b. 5′- UGAGGUAGUAGGUUGUGUGGUU −3′	Integrated DNA Technology	http://www.idtdna.com/pages
let-7c. 5′- UGAGGUAGUAGGUUGUAUGGUU −3′	Integrated DNA Technology	http://www.idtdna.com/pages
let-7d. 5′- AGAGGUAGUAGGUUGCAUAGUU −3′	Integrated DNA Technology	http://www.idtdna.com/pages
let-7e. 5′- UGAGGUAGGAGGUUGUAUAGUU −3′	Integrated DNA Technology	http://www.idtdna.com/pages
let-7f. 5′- UGAGGUAGUAGAUUGUAUAGUU −3′	Integrated DNA Technology	http://www.idtdna.com/pages
let-7g. 5′- UGAGGUAGUAGUUUGUACAGUU −3′	Integrated DNA Technology	http://www.idtdna.com/pages
let-7i. 5′- UGAGGUAGUAGUUUGUGCUGUU-3′	Integrated DNA Technology	http://www.idtdna.com/pages
miR-98. 5′- UGAGGUAGUAAGUUGUAUUGUU −3′	Integrated DNA Technology	http://www.idtdna.com/pages
Mut. Oligo. 5′- UGAGGUAGAAGGAUAUAAGGA −3′	Integrated DNA Technology	http://www.idtdna.com/pages
let-7d mut-N. 5′- AGAGGUAGUAGGUUGUAUAGUU −3′	Integrated DNA Technology	http://www.idtdna.com/pages
let-7e mut-N. 5′- UGAGGUAGGAGGAUGUAUAGUU −3′	Integrated DNA Technology	http://www.idtdna.com/pages
let-7e mut-CS. 5′- AUGAGGAGGAGGUUGUAUAGUU −3′	Integrated DNA Technology	http://www.idtdna.com/pages
mTLR7 forward 5′-ATGTGGACACGGAAGAGACAA-3′, mTLR7 reverse 5′-GGTAAGGGTAAGATTGGTGGTG-3′	Ramirez-Ortiz et al., 2015	https://idp.nature.com/authorize?response_type=cookie&client_id=grover&redirect_uri=https%3A%2F%2Fwww.nature.com%2Farticles%2Fni.3143
TBP forward 5′-AAGGGAGAATCATGGACCAG-3′, TBP reverse 5′- CCGTAAGGCATCATTGGACT-3′	Haage et al., 2019	https://www.sciencedirect.com/science/article/pii/S0889159119304659#t0005

(Continued on next page)

Continued

REAGENT or RESOURCE	SOURCE	IDENTIFIER
Recombinant DNA		
pRRL.PPT.MP.mcherry	this paper	N/A
Software and Algorithms		
LASAF software	Leica Microsystem	https://www.leica-microsystems.com/products/microscope-software/details/product/leica-las-x-ls/
Fiji ImageJ software (1.51m9 64 mb)	NIH	https://imagej.nih.gov/ij/download.html; RRID: SCR_003070
Imaris 6.3.1	Bitplane	http://www.bitplane.com/releasenotes/imaris631.aspx
GraphPad Prism 7	La Jolla	
FlowJo v10 software	Tree Star	http://docs.flowjo.com/d2/
Igor Pro 7 software	Wavemetrics	https://www.wavemetrics.com/order/order_igordownloads7.htm
Microsoft Excel	Microsoft	https://www.microsoft.com/en-us/; RRID:SCR_016137
Other		
HM650V vibratome	Thermo Scientific	cat#10076838
Leica TCS SPE	Leica Microsystem	N/A
LSRII flow cytometer	BD Bioscience	N/A
FACS Aria II flow cytometer	BD Bioscience	N/A
Bio-Plex® 200 System	Bio-Rad	https://www.bio-rad.com/de-de/product/bio-plex-200-systems?ID=715b85f1-6a4e-41b3-b5d9-80202d779e13
gentleMACS™ Octo Dissociator	Miltenyi Biotech	Cat#130-095-937
TECAN Infinite M200	Tecan	https://lifesciences.tecan.com/plate_readers/fluorescence_absorbance_luminescence?p=tab–5

LEAD CONTACT AND MATERIALS AVAILABILITY

Further information and requests for resources and reagents should be directed to and will be fulfilled by the Lead Contact, Prof. Dr. Seija Lehnardt (seija.lehnardt@charite.de). This study did not generate new unique reagents.

EXPERIMENTAL MODEL AND SUBJECT DETAILS

Animals

C57BL/6J (wild-type, WT), as well as $Tlr7^{-/-}$, $Tlr2^{-/-}$ and $Tlr4^{-/-}$ mice were used for microglial primary cultures. Neonatal microglia were isolated from male and female mice, while adult microglia were derived from male mice. For the acute isolation of adult microglia, $Cx3cr1^{GFP/+}$ x $Ccr2^{RFP/+}$ male mice were used. For the generation of primary gliomas using the RCAS/Tv-a system, $Nestin-tv-a;Ink4a-Arf^{-/-};Pten^{fl/fl}$ male mice were employed. For organotypic brain slice cultures, transgenic male mice expressing EGFP under the Csf1r promoter (MacGreen) were used. All animals were maintained and handled in accordance with the German Animal Protection Law and approved by the Regional Office for Health and Social Services in Berlin (Landesamt für Gesundheit und Soziales – LaGeSo, Berlin, Germany).

Human Biopsies

Freshly resected samples from male patients with glioblastoma were provided by the Department of Neurosurgery, Helios Clinic Buch (Berlin, Germany) and the Department of Neurosurgery, University Medical Center Schleswig-Holstein (Kiel, Germany). Brain samples from male patients with epilepsy were provided by the Department of Neurosurgery, Charité-Universitätsmedizin Berlin (Berlin, Germany). The samples used here were small fragments from tissue blocks. The study has complied with all relevant ethical

regulations and was approved by the institutional review boards. Written informed consent was obtained from all patients partici-pating in the study.

Cell Lines
For fluorescence labeling, GL261 cells (Charles River Laboratory, Wilmington, MA, USA) were lentivirally transduced with a plasmid. Briefly, the mCherry gene was cloned into a lentiviral vector on a pRRL backbone (https://www.addgene.org/12252/), downstream of the MP71 promoter. After the production of viral particles, WT GL261 cells were transduced for 24 h at a MOI of 1 by using RPMI medium supplemented with 10% fetal calf serum, 2% Glutamin, 1% antibiotics Penicillin and Streptomycin, and 0.4 mg/ml Polybrene (Merck, Darmstadt, Germany). Transduction was stopped by adding new fresh medium. Mcherry-labeled GL261 cells (information on the sex of origin is unavailable) were selected via FACS cell sorting and frozen until further use.

Primary Cell Cultures
Neonatal primary microglial cultures from WT and TLR2-, TLR4-, and TLR7-deficient mice were prepared as previously described (Ifuku et al., 2016; Prinz et al., 1999). Briefly, brains, including cortex and midbrain, from postnatal day 0-2 (P0-P2) male and female newborns were freed of blood vessels and meninges, mechanically dissociated into 1 mm^3 pieces and digested with 1% trypsin and 0.05% deoxyribonuclease. Digested tissue was further mechanically dissociated with a fire-polished pipette and washed twice in HBSS. Mixed glial cultures were plated and cultured for 9-12 d in Dulbecco's modified Eagle's medium (DMEM) supplemented with 10% fetal calf serum and 1% antibiotics Penicillin and Streptomycin. After 7 d, 33% L292-conditioned medium was added to the cultures, and the microglial cells were isolated by gentle shaking at 37°C for 1 h on a shaker (100 rpm) and plated.

Microglia from adult mice were prepared as described previously (Pannell et al., 2016). In short, brains obtained from adult male mice (P49-56) were freed of blood vessels and meninges, mechanically dissociated, and digested with trypsin and DNase as described for neonatal cultures. After further dissociation cells were plated on a confluent monolayer of P0-P2 astrocytes in 75 cm^2 flasks. The feeder astrocytic layer was depleted of neonatal microglial cells by using chlodronate (200 μg/ml) before plating the microglial cells. Mixed adult and neonatal glial cultures were maintained in fresh complete DMEM, and the medium changed every third day, followed by addition of 33% L292-conditioned medium at day 7. One week later, cells were shaken off and used for experiments within 24-48 h.

Bone marrow-derived macrophages were isolated from WT male adult mice (P49-59) as previously described (Manzanero, 2012). Mice were sacrificed by cervical dislocation, and their back legs were removed by cutting near the pelvic area. The skin was removed together with muscles, and ligaments, and the bone was cut below the ankle joint. The femur and tibia were isolated by slightly bending the knee joint. Complete RPMI 1640 tissue culture medium, supplemented with 10% heat-inactivated fetal bovine serum and 1% antibiotics, was flushed through the bone, and the contents collected into a sterile 15 mL polypropylene tube. After centri-fugation for 5 min at 1200 rpm, red blood cells were lysed by adding Erylyse Buffer for 3 min and subsequently centrifuged for 5 min at 1200 rpm. Cells were then passed through a 70 μm cell strainer and plated in 10 cm dishes with fresh complete RPMI medium supplemented with 2 ng/ml of M-CSF to allow differentiation into macrophages. After 7 d, cells were trypsinized and used for exper-iments within 1 d of plating.

METHOD DETAILS

Isolation of Fresh Naive Adult Microglia and GAMs for Functional Assays
Microglia were isolated from healthy or GL261 tumor-bearing Cx3cr1$^{GFP/+}$ x Ccr2$^{RFP/+}$ male mice (P84). Mice were fully anaesthetized with Narcoren (Merial GmbH, Hallbergmoos, Germany) and transcardially perfused with ice-cold 1x Phosphate Buffered Saline (PBS). Brains were extracted, excluding the brain stem and cerebellum, and digested into a single cell suspension by using Adult Brain Dissociation Kit mouse and rat (Miltenyi Biotech GmbH, Bergisch Gladbach, Germany) according to the manufacturer's manual. Briefly, the kit consists of one enzymatic digestion step by using gentleMACS^{TM} Dissociator with heaters followed by a debris and myelin removal step. Dissociated cells were directly isolated via Fluorescent-activated cell sorting (FACS) by using FACS Aria flow cytometer (BD Biosciences, San Jose, USA). The gating strategy used the GFP/RFP ratio from the reporter mice. Mi-croglia, defined as the GFP^{high}RFP$^-$ population, and invading macrophages, defined as the GFP^{high}RFP$^+$ population, were sorted in fresh complete DMEM supplemented with antimycotics and antibiotics. Following centrifugation at 500 g for 5 min, 5x10^4 microglial cells were plated in a 96-well-plate, and used for experiments 24 hr later.

Microglia and astrocytes from P14 and 12-week-old WT male mice were isolated via FACS sorting by using the following dye-coupled antibodies: CD11b, CD45 (eBioscience, San Diego, USA), and ACSA2 (Miltenyi Biotech GmbH, Bergisch Gladbach, Germany).

let-7 miRNA Stimulation and TNF-α Enzyme-Linked Immunosorbent Assay
To test *let-7* miRNA-mediated cell activation *in vitro*, we stimulated cells, collected the supernatant and tested for TNF-α release via an ELISA assay. Neonatal and adult primary microglia as well as bone marrow-derived macrophages were plated into a 96-well-plate at a density of 3x10^4 cells per well in 150 μl medium, while acutely isolated adult microglia were plated in a 96-well-plate at a density of 5x10^4 cells per well. To assess the time course, cells were stimulated with 660 nM of *let-7* oligoribonucleotide for 9 h, 24 h and 30 h. To

characterize the dose response, cells were stimulated for 24 h with increasing concentrations of the respective miRNA (1, 5 and 10 μg/ml corresponding to 132, 660, and 1320 nM, respectively). At the appropriate time point, supernatants were collected and tested for TNF-α concentration, expressed in ng/ml, using an enzyme immunosorbent assay (ELISA) and the mouse TNF alpha ELISA Ready-SET-Go!™ kit (Affymetrix eBioscence, San Diego, CA, USA) according to the manufacturer's manual. For treatment of GL261 cells with microglial conditioned medium (MCM), microglia were plated in a 6-well-plate at a density of 1x10⁶ cells per well and stimulated with 5 μg/ml *let-7b* or *let-7d* oligoribonucleotide for 24 h.

Multiplex Immune Assay
Detection of cytokines in supernatants collected from microglial cell cultures stimulated over time with *let-7* miRNA family members was performed using the ProcartPlex mouse Multiplex Immunoassay Mix&Match (Affymetrix eBioscience, Vienna, Austria) according to the manufacturer's manual. Briefly, the magnetic beads-based assay enables the simultaneous detection and quantification of multiple proteins in a single sample. Prior to incubation, samples were vortexed followed by centrifugation to remove particles. Detection of the proteins was performed by using Luminex 200. Analysis was performed by using Bioplex System Software 4.0 (Bio-Rad, Hercules, CA, USA). The cytokine analysis included TNF-α, IL-6, IL-10, IL-1β, GRO-α, MIP-2, RANTES, GM-CSF, IP-10, MCP-1, MCP-3, MIP-1α, and MIP-1β. Expression levels are shown as Mean Fluorescent Intensity (MFI).

Agarose Spot Assay
Agarose spot assay was performed as previously described (Wiggins and Rappoport, 2010). In summary, 0.1 g of low-melting point agarose (Promega, Madison, WI, USA) was diluted in 20 mL of PBS originating 0.5% agarose solution. The solution was then heated until boiling and subsequently cooled down to 40°C. Afterward, 90 μl of agarose solution was mixed with 10 μl of PBS with or without *let-7* miRNAs (at a concentration of 660 nM) in a 0.5 mL Eppendorf tube. 10 μl of mixed solution were rapidly plated into 35 mm glass bottomed dishes (Maktek Corporation, Ahland, MA, USA) and were cooled down for 10 min at 4°C. Four spots were pipetted in one dish, two containing PBS only and two with selected *let-7* oligonucleotides. 5x10⁵ microglia cells from WT or *Tlr7⁻/⁻* mice were plated in the dish in 2 mL DMEM supplemented with 10% fetal calf serum and incubated at 37°C for 3 h. Subsequently, the cells inside the spot were counted under the microscope. To assess microglial motility, we also applied the respective oligoribonucleotide to the medium. For chemotaxis assays, *let-7* oligoribonucleotides or mutant oligoribonucleotide, with or without RNase A (10 μg) pre-treatment, were only present inside the spot.

Flow Cytometry Analysis
Neonatal primary microglial cultures from WT and *Tlr7⁻/⁻* mice were prepared as previously described (see above) and seeded at a confluency of 5x10⁵ cells in a 35 mm Petri dish. Microglia were stimulated with *let-7b*, *let-7d* and *let-7e* (660 nM) for 24 h followed by cell collection by scratching in ice-cold PBS and centrifugation at 500 g for 5 min at 4°C. The cell pellet was resuspended in ice-cold FACS buffer (PBS supplemented with 1% fetal calf serum) and divided in two groups (each group contained 2x10⁵ cells), for immunolabeling with the following dye-coupled monoclonal anti-mouse antibodies: CD45, CD11b, MHC I, MHC II and CD54 (eBioscience, San Diego, USA) for 20 min at 4°C. Next, cells were immediately acquired on a LSRII flow cytometer (BD Bioscience, San Jose, USA), and the data analyzed using FlowJo v10 software (Tree Star). Expression values are shown as MFI normalized to unstimulated control condition.

Tumor Injection *In Vivo*
Tumors were inoculated *in vivo* as previously described (Szulzewsky et al., 2015). Injections were performed using a stereotactic frame (Stoelting, Wood Dale, IL, USA). Mice used for these experiments were 8-14-week old (C57BL/6 mice and *Cx3cr1^GFP/+^x Ccr2^RFP/+^* for GL261 cell injection, *C57BL7/6* mice for RCAS-PDGFb tumor cell re-implantation) or 4.5-10-week-old (*Ntv-a/Ink4a-Arf⁻/⁻* mice for DF-1 RCAS-PDGFb injection). Mice were anaesthetized with intraperitoneal injections of ketamine (0.1 mg/g, Pharmazeutischen Handelsgesellschaft, Garbsen, Germany) and xylazine (0.02 mg/g, Bayer, Leverkusen, Germany). Animals were also treated with 0.25% Marcaine (volume about 0.1 ml/25 g) administered right before the surgery.

One microliter cell suspensions (2x10⁴ GL261 cells, 4 × 10⁴ transfected DF-1 cells, or 5x10⁴ RCAS-PDGFb tumor cells) were delivered using a 30-gauge needle attached to a Hamilton syringe (Hamilton, Reno, NV, USA). Coordinates for GL261 injections into C57BL/6 mice were bregma 1 mm anterior, Lat (lateral) −2 mm (right of midline), and a depth −3 mm from the dural surface. Coordinates for injections of DF-1 cells and RCAS-PDGFb tumor cells into *Ntv-a/Ink4a-Arf⁻/⁻* mice and *C57BL/6* mice, respectively, were bregma 1.5 mm anterior, Lat −0.5 mm, and a depth 2.0 mm. Mice were monitored daily for the first two weeks and twice a day starting from day 15 post-injection for symptoms of tumor development (lethargy, hydrocephalus, head tilting). At day 18-19 and day 30 for GL261 and RCAS, respectively, animals were sacrificed and perfused with 1x PBS followed by decapitation and brain resection.

Total RNA Extraction and Quantitative RT-PCR
For *let-7* expression analysis in human and murine brain samples, we extracted total RNA with the mirVana™ PARIS™ kit (Thermo Fisher Scientific, Waltham, MA, USA), according to the manufacturer's protocol. Briefly, human and murine brain samples were processed frozen and disrupted by using a mortar and pestle in a bed of dry ice. The tissue powder obtained was scraped and mixed

rapidly into Cell Disruption Buffer. The mixture was then homogenized by using Ultra-Turrax® (Merck, Darmstadt, Germany) at 21.500 rpm for 30 s. Once the lysate was homogenized, equal volume of 2x denaturing solution and incubated on ice for 5 min. Next, the sample lysate plus 2x denaturing solution was mixed with an equal volume of Acid-Phenol:Chloroform and vortexed for 60 s. After a centrifugation step of 5 min at maximum speed at room temperature, the upper aqueous phase was collected and transferred to a new tube. 1.25 volumes 100% ethanol were added to the aqueous phase, and the mixture was placed into the filtered column and centrifuged for 30 s at 10.000 g at room temperature. The column was then washed with miRNA Wash Solution 1 and 2/3 and ultimately eluted with RNase free water. Total RNA amount was quantified with the Thermo Scientific™ Nanodrop™ One spectrophotometer (Thermo Fisher Scientific, Waltham, MA, USA). Reverse transcription and quantitative PCR was performed using the TaqMan® MicroRNA Assay, according to the manufacturer's manual. Taqman PCR reactions were performed in the Step one Plus Real Time PCR system (Applied Biosystems, Foster City, CA, USA). Expression data were normalized to *miR-16* for each sample.

For detection of TLR7 expression in freshly isolated microglia, astrocytes, and the tumor cell lines GL261 and RCAS, cDNA was obtained using the SuperScript II reverse transcriptase (Invitrogen, Carlsbad, CA, USA) with oligo-dT primers (Invitrogen, Carlsbad, CA, USA) according to the manufacturer's instructions. Quantitative real-time PCR was performed in a 7500 Fast Real-Time thermocycler (Applied Biosystems, Foster City, CA, USA) using SYBR select Master Mix (Applied Biosystems, Foster City, CA, USA). TATA-binding protein (TBP) was used as housekeeping gene. The following primers (synthesized by Biotez GmbH, Berlin, Germany) were used: mTLR7 forward 5′-ATGTGGACACGGAAGAGACAA-3′, mTLR7 reverse 5′-GGTAAGGGTAAGATT GGTGGTG-3′, TBP forward 5′-AAGGGAGAATCATGGACCAG-3′, TBP reverse 5′- CCGTAAGGCATCATTGGACT-3′.

Analysis of Cell Viability and Apoptosis in GL261 Cells

GL261 cells were treated with microglial conditioned medium (MCM) stimulated with select *let-7* oligoribonucleotides, as indicated in the Figure legend, and cell viability and apoptosis rate were assessed. For viability assay, GL261 cells were plated in a 96-well-plate at a density of 1×10^4 cells/well and treated with 100 μl of *let-7*-stimulated MCM for 24, 48 and 96 h. At each time point, 10 μl of Cell Counting Kit-8 (CCK8, Tebu-Bio, Offenbach, Germany) reagent was added. After 2 h, absorbance was measured at 450 nm on a microplate reader (TECAN). Values were normalized to the unstimulated condition. For cell death analysis, GL261 cells were plated in a 24-well-plate at a density of 5×10^4 cells/well and treated with 300 μl of *let-7*-stimulated MCM for 48 h. Subsequently, cells were fixed in 4% PFA and analyzed by TUNEL assay and immunostaining employing an antibody against activated caspase-3 (see below).

Organotypic Brain Slice Cultures

Organotypic brain slice preparation was performed as previously described (Markovic et al., 2005). Briefly, brains derived from P14-16 MacGreen animals were removed and placed in ice-cold PBS. Cerebellum and olfactory bulb were removed, and the fore-brain was placed on a glass block and cut in the coronal plane into 250 μm sections with a vibratome (Microm HM650V, Thermo Scientific, Waltham, MA, USA). Brain slices were transferred onto 0.4 μm polycarbonate membranes in the upper chamber of a transwell tissue insert (Falcon model 3090, Becton Dickinson, Franklin Lakes, NJ, USA), which was inserted into a 6-well-plate (Falcon model 3502, Becton Dickinson, Franklin Lakes, NJ, USA). To ensure the same experimental conditions three slices, representing three different brain areas, were mounted on each insert. Thereafter, brain slices were incubated in 1 mL of culture medium per well containing DMEM supplemented with 10% heat-inactivated fetal bovine serum (Atlanta Biological, Norcross, GA), 0.2 mM glutamine, 100 U/ml penicillin, and 100 mg/ml streptomycin (medium-1). After overnight equilibration of the brain slices in medium-1, slices were incubated with cultivation medium-2. Medium-2 contained 25% heat-inactivated horse serum, 50 mM sodium bicarbonate, 2% glutamine, 25% Hank's balanced salt solution, 1 mg/ml insulin, 5 mM Tris (all from Life Technologies, Carlsbad, CA, USA), 2.46 mg/ml glucose (Braun Melsungen, Germany), 0.8 mg/ml vitamin C, 100 U/ml penicillin and 100 mg/ml streptomycin (all from Sigma-Aldrich, St. Louis, MO, USA) in DMEM (GIBCO, Thermo Fisher Scientific, Waltham, MA, USA). Slices were maintained in culture for 5 d with medium change every two days.

Tumor Cell Injection into Brain Slices and let-7 miRNA Treatment

One day after sectioning, 5000 cultured mCherry GL261 glioma cells in a volume of 0.1 μl were injected into the slices using a micro-syringe mounted to a micromanipulator. An injection canal was formed that reached 150 μm deep into the 250-mm-thick slice. The needle was then retracted by 50 μm, leaving an injection cavity of approximately 50 μm where the tumor cell suspension was slowly inoculated over 30 s. Afterward, the syringe was pulled out in 10 μm incremental steps over 60 s. To ensure identical experimental conditions, gliomas were always inoculated in the striatal area of both hemispheres. In parallel to tumor inoculation, the *let-7* miRNAs complexed with Lyovec were added to the medium at a concentration of 0,5 μg/ml and replenished when fresh new medium was changed so that the *let-7* oligoribonucleotides were constantly present.

Depletion of Microglia

For microglial depletion, clodronate-loaded liposomes (Liposoma, Amsterdam, Netherlands) were used. Brain slices were incubated with the liposomes for 24 h at 37°C. Afterward, slices were incubated with medium-2 (see above) for equilibration, with glioma cell injections occurring at least two days later.

Immunofluorescence, Confocal Microscopy, and Tumor 3D Reconstruction

GL261 cells seeded on coverslips and treated with *let-7*-stimulated MCM were fixed for 10 min in 4% PFA, washed 3x with PBS and incubated for 1 h at room temperature in permeabilization/blocking solution (5% normal donkey serum and 0.2% Triton X-100 D-PBS). Subsequently, anti-rabbit activated caspase-3 antibody was added to the permeabilization/blocking solution (1:300), and cells were incubated at 4°C overnight. This step was followed by adding DAPI solution (1:5000; Sigma-Aldrich, St. Louis, MO, USA) and donkey anti-rabbit Alexa Fluor 647 (1:500) incubation at room temperature. Afterward, coverslips were mounted and analyzed at the confocal microscope. For TUNEL analysis, *In Situ* Cell Death Detection Kit, Fluorescein (Roche, Basel, Switzerland) was used, according to the manufacturer's manual. Briefly, cells were permeabilized and blocked in a D-PBS solution containing 0.1% sodium citrate and 0.1% Triton X-100 for 3 min on ice. Afterward, cells were incubated with the TUNEL reaction mixture for 1 h at 37°C, followed by 3x washing with D-PBS, and incubation with DAPI solution, before mounting on a glass slide.

Organotypic brain slices were fixed at day 4 post-injection with 4% PFA for 1 h followed by PBS washing and incubation overnight at 4°C with D-PBS supplemented with 5% donkey serum and 0.3% Triton X-100. Slices were incubated with anti-rabbit activated caspase-3 primary antibody (1:100) for 24 h followed by 3x washing with D-PBS. Incubation with donkey anti-rabbit Alexa Fluor 647 secondary antibody (1:250) was performed for 2 h at room temperature. In addition, staining with DAPI was performed for 2 h. For TUNEL staining, ApopTag Plus Fluorescein *In Situ* Apoptosis Detection Kit (Merck, Darmstadt, Germany) was used following the manufacturer's instructions. Briefly, after 1 h fixation in 4% PFA, slices were incubated for 10 min at room temperature with permeabilization buffer containing ethanol: acetic acid, 2:1 (v:v). Slices were incubated for 1 min with equilibration buffer and subsequently incubated with the TUNEL reaction mixture (TdT enzyme and reaction buffer) for 2 h at 37°C in a humidified chamber. The reaction was stopped by incubating the slices with the stop/wash buffer for 15 min at room temperature. Finally, anti-digoxigenin-conjugated solution was applied on the slices for 30 min at room temperature. Slices were mounted for tumor volume quantification and apoptosis analysis. Tumor volumes were determined by using the confocal laser microscopy scanning (Leica TCS SPE, Leica Microsystems, Wetzlar, Germany). We acquired images with a 20x oil immersion objective by using a z stack with a 2 μm step size interval and tile scan mode. Data analysis to assess tumor volume was performed by using Imaris 9 (Bitplane, Zürich, Switzerland). Tumor volumes of high-resolution SPE confocal microscopy stacks were 3D rendered by application of 1 μm object detail, 15 threshold background and 1000 tridimensional pixels (voxels). The surface objects obtained were unified in one single object, and volume mean values were extracted.

For apoptosis quantification *in vitro* and *ex vivo*, we acquired 4 images per coverslip/tumor at 20x and quantified by ImageJ software with the additional threshold adjustment tool and cell counter plug in.

QUANTIFICATION AND STATISTICAL ANALYSIS

All experiments were performed at least three times, and all data were represented as mean ± SEM. We assessed statistical significance by using Prism 7 Windows (GraphPad Software, San Diego, CA, USA). For ELISA and multiplex analysis we used Kruskal-Wallis test followed by Dunn's multiple comparison post hoc test. For migration studies, FACS analysis, viability/cell death analysis, and comparison between organotypic brain slices, one way ANOVA followed by Bonferroni post hoc test, was performed. For paired comparison in human and mouse quantitative PCR analysis, Mann Whitney *U* test or one way ANOVA followed by Dunnett's multiple comparison post hoc test was performed. Significance was set at p < 0.05.

DATA AND CODE AVAILABILITY

All data generated within this study are provided with the Figures and Supplemental information.